Doctoral Thesis

Synthesis and Conformation of Optically Active Polyurethanes Based on 1,1’-Bi(2-naphthol)

(1,1’-ビ(2-ナフトール)に基づく光学活性ポリウレタンの合成とコンホメーション)

Heshuang Dai（戴 河双）

Hokkaido University

Contents

Chapter 1. General Introduction

1.1 Background

Chirality of polymer chain plays crucial roles in various material applications, and helical conformation has been a most important focus in this research discipline. Helix is a chiral shape of a chain which may be right- or left-handed, and a material consisting of single-handed helices or preferred-handed helices may exhibit chiroptical properties. Many natural polymers are single-handed helical as represented by proteins (peptides), DNAs, and polysaccharides where single-handedness is controlled by handedness of centers of chirality in the monomeric unit.

As for synthetic polymers, helicity of polymer chain can be introduced by designing monomer and polymerization reaction and by controlling interactions of random chain with external molecule. Single-handed or preferred-handed helix can be created on the basis of chirality of ligand or monomeric units or external molecules. Optically active, helical synthetic polymers find various functions including chiral recognition of racemates,[1] asymmetric catalysis,[2] optical non-linearity,[3] chiroptical switch,[4] and circularly polarized luminescence.[5] this chapter introduces the background of synthetic helical polymers.

1.2 Synthetic, Helical Polymers

Following the early and important studies on helical structures of natural macromolecules including polysaccharide (α-amylose) (1936),[6] polypeptides (1951),[7] and DNAs (1953),[8] research aiming at synthetic helical polymers came into bloom. The first synthetic helix was made for isotactic polypropylene by Natta in 1955 where the helix was racemic and was stable only in the solid state.[9] Later, preferred-handed helix of

isotactic polyolefins which can be maintained in solution was realized based on the effect of side-chain chirality.[10] Further, a break-through in this field was made in 1979, *i.e.*, single-handed helical, isotactic poly(triphenylmethyl methacrylate) (poly(TrMA)) was synthesized by asymmetric anionic polymerization (asymmetric helix-chirogenic polymerization) using chiral ligand as chirality source;[11] this polymer is the first example of single-handed helical polymer having no configurational chirality.

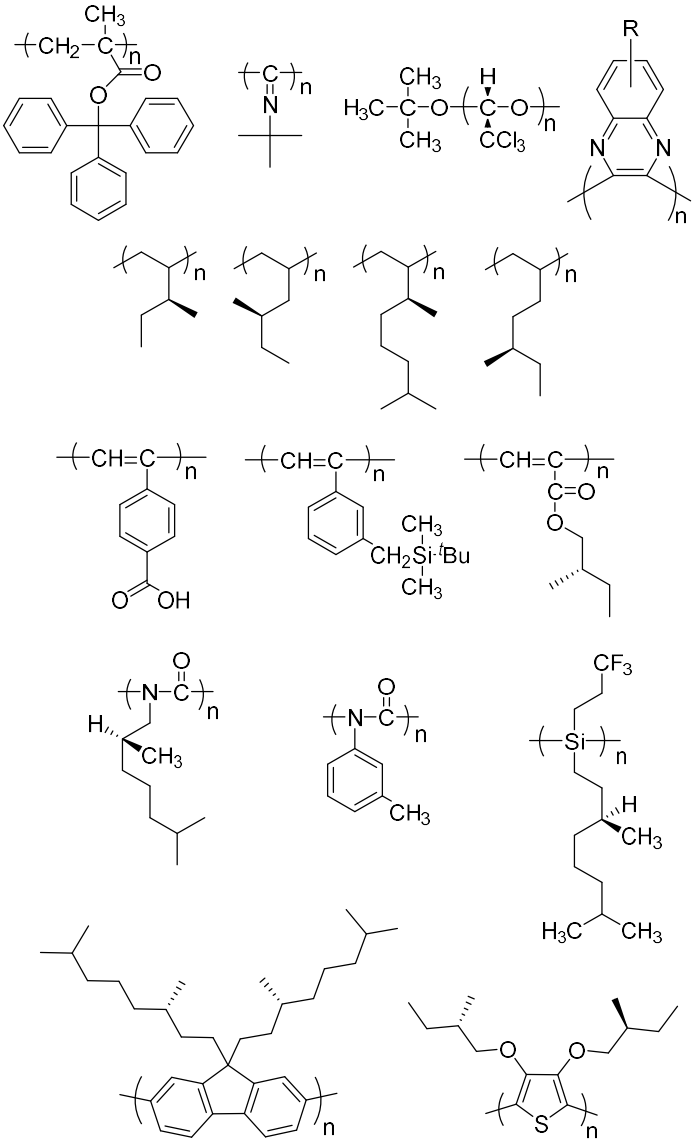

Fig. 1. Examples of synthetic helical polymers.

This polymer can hold its single-handed helical conformation through steric repulsion between the bulky side-chain groups. Examples of other synthetic helical polymers include polyolefins,[10] polyisocyanates,[12] polyisocyanides,[13] polychloral,[14] poly(meth)acryaltes,[15] polysilanes,[16] polyacetylenes,[17] and other main-chain conjugated polymers (**Fig. 1**).[18]

1.3 Methods to Create Optically Active, Helical Polymers

Optically active, helical polymers can be prepared by helix-sense-selective polymerization (asymmetric helix-chirogenic polymerization) of a monomer designed to form a helical chain where chiral ligand can induce single-handed helicity. The polymerization is conducted typically using an anionic initiator or a transition metallic catalyst under critically controlled conditions. The overall process of the production of is rather laborious and expensive. In order to effectively explore potential functions and properties of optically active, helical polymers, less demanding ways of synthesis would be desirable. One of such methods is to polymerize optically active monomers into optically active polymers where chirality of the monomer is intact, and helicity is induced as a new structural element to the polymer based on the chirality of the monomer. If this method is combined with a chemically simple technique of polymerization, a significantly facile way of the synthesis of optically active, helical polymers.

1.4 Synthesis of Chiral Polyurethanes by Polyaddition

A chemically simplest method of polymerization may be polyaddition leading to polyurethanes. Polyurethanes can be prepared by polyaddition of polyols and

polyisocyanates and are widely used in variety of disciplines including architecture, automotive applications, textile, electronics, aviation, national defense, and medical technologies. Based on the variation of monomers for polyurethanes, they can be rigid or flexible or thermoplastic and they can be hydrophobic or hydrophilic. Polyurethane materials showing such different properties have been widely used as binders, coating, adhesives, sealants and elastomers.[19] Development of polyurethane originates in Germany and was initiated in 1937 by Otto Bayer and his colleagues.[20] They studied the polymerization of diisocyanate and found the formation of various polyurethane and polyurea compounds but without value. Bayer then made rigid foam, paint and adhesive during World War II, and American enterprises began to produce rigid foam.[21] After 1950s, polyurethane foam began to be industrially produced. Since then, polyurethane elastomer, polyurethane coating, polyurethane adhesive, polyurethane elastic fiber and so on were successfully synthesized in industries,[21-24] and continuing improvement gradually made the production process of polyurethane materials matured. As a result, polyurethane materials have risen rapidly in the chemical industry.[24-29]

Polyaddition systems leading to chiral polyurethanes have been only rarely reported[30,31] in spite of their simplicity in procedure. As representative examples, there haven been two articles published about optically active polyurethane synthesis by polyaddition between 1,4-diisocyanatobezene (14DIB) and optically active 2,2'-dihydroxy-1,1'-binaphthyl (BINOL) yielding poly(BINOL-*alt*-14-DIB) (Scheme 1). The first synthesis was reported in 2009 by a Chinese group. While in this report, detailed results of the polyaddition were not shown, and helical conformation of the polymer was not elucidated at all, the polymer was shown to exhibit moderate chiral resolution ability toward small-molecular racemic compounds.[30] In 2015, a Hokkaido

University group disclosed that the polyaddition between (*R*)-BINOL at 100% e.e. and 14DIB leads to a 2/1-helical polymer in addition to a significant amount of cyclic dimer (Scheme 1).[31] The BINOL-14DIB polyaddition system was also found to form cyclic trimer as well as the cyclic dimer. The helical structure of the polymer was supported by circular dichroism (CD) spectra which suggest the chiral alignment of the -C(O)-NH-C_6H_4-NH-C(O)- moieties and XRD profiles which indicated the formation of π-stacking of the same moieties as well as molecular dynamics simulations. The value of this work is on the following aspects: (1) a helical structure was explicitly studied for a chiral polyurethane and (2) the conformation proposed for the polymer was a 2/1-helix which had been known only for a limited number of vinyl and diene polymers.

With such conformational information in hand, one may assume that the aforementioned chiral recognition ability may arise from enantiomer-selective interactions between small-molecular racemic compounds with the rigid helical chain.

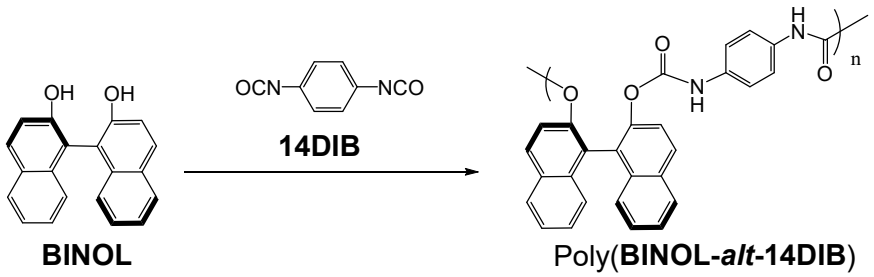

Scheme 1. Polyaddition between 1,4-diisocyanatobezene and optically active BINOL.

1.5 Aims and Achievements in This Work

In this work, as a most facile method of helical polymer synthesis, polyaddition between (*R*)- or (*S*)-2,2'-dihydroxy-1,1'-binaphthyl (1,1'-bi(2-naphthol), BINOL), a

chiral diol monomer, and a diisocyanate monomer leading to polyurethane is studied in detail (Scheme 2).

Scheme 2. Syntheses of polyurethanes from BINOL and diisocyanates.

In the polyurethane synthesis based on BINOL, single-handedness is controlled by single-handed (*R*)- or (*S*)- BINOL. BINOL has been known to be a robust and versatile, chiral organic backbone and used as a structural motif for various chiral polymers. This work proposes a concept of simple, modular synthesis of functional, helical polymers based on BINOL and various diisocyanates. Diisocyanates can be synthesized from corresponding diamines through reactions with triphosgene. By choosing a proper diisocyanate, desired functional group ("-**R**-" in Scheme 1) can be incorporated monomer unit in a helical chain. This method is superior over the other methods of functional helix synthesis from a view of facileness of experimental procedure.

This work focuses on the following two aspects of chiral polyurethane synthesis based on BINOL. The first point is the effect on e.e. of BINOL. Unlike the preceding report,[31] BINOL at various e.e.'s is used in this work to investigate the effects of e.e. on polymerization behaviors and polymer structure. In polymer systems, chirality is often significantly amplified. Representative examples have been reported for polyisocyanate systems where single-handed, dynamic helicity is induced by the effects of chiral side-

chain group whose e.e. is quite low ("majority rule").[32] In the polyisocyanate cases, interactions between side-chain groups are proposed to induce single-handed helix. With such background, it is expected that amplification effects may lead to a large bias of helicity even at a rather low e.e. of BINOL through cooperation among BINOL units with the same hand of chirality. The polyurethanes would have a rather static, stable helix unlike polyisocyanates. Amplification would hence occur, not for the already existing polymer chain in a thermodynamic sense, but for each addition reaction steps in a kinetic sense. If amplification ever takes place, either (R)- or (S)-BINOL would be preferentially incorporated into the polymer chain through addition reaction with an isocyanate group to form urethane bonding. The extent of preference would exceed one expected based on the concentration bias of either enantiomer.

The second point is to demonstrate an example of facile synthesis of a chiral, functional polyurethane. In order to achieve this point, a polyurethane was prepared from 2,7-diisocyanatofluorene. As fluorene is a fluorescent compound, a chiral polyurethane bearing fluorene units may be useful as a material emitting circularly polarized light (CPL). Fluorene units can be part of a helical chain, and hence, they would be in a chiral environment; they would help construction and maintenance of helix, and at the same time, they have a function of light emission. The synthesis can start from commercially available 2,7-diaminofluorene which can be readily transformed to 2,7-diisocyanatofluorene through the reaction with triphosgene, and its polyaddition with BINOL will yield a chiral, emitting polyurethane. In a sharp contrast, if a helical vinyl polymer bearing fluorene in the side chain is a target compound, one would need to synthesize a proper, bulky, helix-forming acrylic monomer that could take multiple steps of chemical reactions as well as purification processes and then would need to find suited

helix-sense-selective polymerization conditions including an adequate chiral ligand which can lead to single-handed helix. Compared with such a procedure to synthesize a functional, helical vinyl polymer, polyaddition systems have a clear advantage of facileness and simplicity.

The contents of each chapter of this thesis follow:

Chapter 1 introduces the background of this thesis work encompassing the background including from the classic methods of chiral polymer synthesis.

Chapter 2 describes the synthesis, structure, and properties of an optically active polyurethane prepared by polyaddition between 1,4-diisocyanatobezene and (*R*)- or (*S*)-BINOL at varous enantiomeric excesses. The polymerization lead to a linear, helical polymer as well as cyclic dimers. The enantiomer of BINOL in excess was more predominantly incorporated into the chain than expected from the ration of concentrations of the two enantiomers. Left-handed helicity was governed by (R)-BINOL, and (S)-BINOL units as minority enantiomeric monomeric units appeared to be a part of left-handed helix.

Chapter 3 presents the synthesis, structure, and properties of an optically active polyurethane prepared by polyaddition between 1,3-diisocyanatobezene and (*R*)- or (*S*)-BINOL at various enantiomeric excesses. Unlike the polyaddition using 1,4-diisocyanatobezene, the reaction led mainly to a linear, helical polymer and a linear dimer species. The polymerization lead to a linear, helical polymer as well as cyclic dimers. The selection between the enantiomers of BINOL was not so clear as that in the case with

1,4-diisocyanatobezene

Chapter 4 discusses the synthesis of structure, and properties of an optically active polyurethane prepared by polyaddition between 2,7-diisocyanatofluorene and optically pure (*R*)- or (*S*)- BINOL. The synthesis targeted a fluorescent polyurethane having fluorene-2,7-diyl units incorporated into the chain which may potentially be useful in emitting polarized light. Two variations of relative orientation of fluorene units were found and controlled, leading to parallel and anti-parallel helical chains.

Chapter 5 describes the general conclusion of this this overviewing the results and discussions of the three chapters.

References

(1) (a) Yuki, H.; Okamoto, Y.; Okamoto, I. *J. Am. Chem. Soc.* 1980, **102**, 6356-6358; (b) Okamoto, Y.; Honda, S.; Okamoto, I.; Yuki, H.; Murata, S.; Noyori, R.; Takaya, H. *J. Am. Chem. Soc.* 1981, **103**, 6971-6973; (c) Okamoto, Y.; Hatada, K. *J. Liq. Chromatogr.* 1986, **9**, 369-384; (d) Nakano, T. *J. Chromatogr. A* 2001, **906**, 205-225; (e) Shimomura, K.; Ikai, T.; Kanoh, S.; Yashima, E.; Maeda, K. *Nature chemistry* 2014, **6**, 429-434.

(2) (a) Reggelin, M.; Schultz, M.; Holbach, M. *Angew. Chem. Int. Ed.* 2002, **114**, 1684-1687; (b) Trindade, A. F.; Gois, P. M. P.; Afonso, C. A. M. *Chem. Rev.* 2009, **109**, 418-514; (c) Yamamoto, T.; Suginome, M. *Angew. Chem. Int. Ed.* 2009, **48**, 539-542; (d) Boersma, A. J.; Coquière, D.; Geerdink, D.; Rosati, F.; Feringa, B. L.; Roelfes, G. *Nature chemistry* 2010, **2** , 991-995; (e) Yamamoto, T.; Yamada, T.; Nagata, Y.; Suginome, M. *J. Am. Chem. Soc.* 2010, **132** , 7899-7901; (f) Tang, Z.; Iida, H.; Hu, H.-Y.; Yashima, E. *ACS Macro Lett.* 2012, **1**, 261-265.

(3) Prasad, P. N. Polymeric materials for non-linear optics and photonics. *Polymer* 1991, **32**, 1746-1751.

(4) (a) Hida, N.; Takei, F.; Onitsuka, K.; Shiga, K.; Asaoka, S.; Iyoda, T.; Takahashi, S. *Angew. Chem. Int. Ed.* 2003, **115** , 4485-4488; (b) Gomar‐Nadal, E.; Veciana, J.; Rovira, C.; Amabilino, D. B. *Adv. Matter.* 2005, **17**, 2095-2098; (c) Gomar-Nadal, E.; Mugica, L.; Vidal-Gancedo, J.; Casado, J.; Navarrete, J. T. L.; Veciana, J.; Rovira, C.; Amabilino, D. B. *Macromolecules* 2007, **40**, 7521-7531; (d) Iida, H.; Mizoguchi, T.; Oh, S.-D.; Yashima, E. *Polym. Chem.* 2010, **1**, 841-848.

(5) (a) Peeters, E.; Christiaans, M. P.; Janssen, R. A.; Schoo, H. F.; Dekkers, H. P.; Meijer, E. *J. Am. Chem. Soc.* 1997, **119**, 9909-9910; (b) Meskers, S.; Peeters, E.; Langeveld‐Voss, B.; Janssen, R. *Adv. Matter.* 2000, **12**, 589-594; (c) Oda, M.; Nothofer, H. G.; Lieser, G.; Scherf, U.; Meskers, S.; Neher, D. *Adv. Matter.* 2000, **12**, 362-365; (d) Nakano, Y.; Fujiki, M. *Macromolecules* 2011, **44**, 7511-7519; (e) Watanabe, K.; Sakamoto, T.; Taguchi, M.; Fujiki, M.; Nakano, T. *Chem. Commun.* 2011, **47**, 10996-10998; (f) San Jose, B. A.; Yan, J.; Akagi, K. *Angew. Chem. Int. Ed.* 2014, **126**, 10817-10820.

(6) (a) Hanes, C. S. *New Phytologist* 1937, **36**, 189-239; (b) Freudenberg, K.; Schaaf, E.; Dumpert, G.; Ploetz, T. *Naturwissenschaften* 1939, **27**, 850-853.

(7) Pauling, L.; Corey, R. B. *Proc. Natl Acad. Sci. USA* 1951, **37**, 729-740.

(8) Watson, J. D.; Crick, F. H. C. *Nature* 1953, **171**, 737-738.

(9) Natta, G.; Pino, P.; Corradini, P.; Danusso, F.; Mantica, E.; Mazzanti, G.; Moraglio, G. *J. Am. Chem. Soc.* 1955, **77**, 1708-1710.

(10) Pino, P.; Lorenzi, G. P. *J. Am. Chem. Soc*. 1960, **82** , 4745-4747.

(11) Okamoto, Y.; Suzuki, K.; Ohta, K.; Hatada, K.; Yuki, H. *J. Am. Chem. Soc.* 1979, **101**, 4763-4765.

(12) (a) Green, M. M.; Andreola, C.; Munoz, B.; Reidy, M. P.; Zero, K. *J. Am. Chem. Soc.* 1988, **110**, 4063-4065; (b) Okamoto, Y.; Matsuda, M.; Nakano, T.; Yashima, E. *J. Polym. Sci., Part A: Polym. Chem.* 1994, **32** , 309-315.

(13) Kamer, P. C. J.; Nolte, R. J. M.; Drenth, W. *J. Am. Chem. Soc.* 1988, **110**, 6818-6825.

(14) Ute, K.; Hirose, K.; Kashimoto, H.; Hatada, K.; Vogl, O. *J. Am. Chem. Soc*. 1991, **113**, 6305-6306.

(15) Okamoto, Y.; Suzuki, K.; Ohta, K.; Hatada, K.; Yuki, H. *J. Am. Chem. Soc.* 1979, **101**, 4763-4765.

(16) Fujiki, M. *J. Am. Chem. So*c. 1994, **116** , 11976-11981.

(17) (a) Yashima, E.; Huang, S.; Matsushima, T.; Okamoto, Y. *Macromolecules* 1995, **28** , 4184-4193; (b) Yashima, E.; Matsushima, T.; Okamoto, Y. *J. Am. Chem. Soc.* 1997, **119**, 6345-6359; (c) Nakako, H.; Nomura, R.; Tabata, M.; Masuda, T. *Macromolecules* 1999, **32**, 2861-2864; (d) Nakako, H.; Mayahara, Y.; Nomura, R.; Tabata, M.; Masuda, T. *Macromolecules* 2000, **33**, 3978-3982.

(18) (a) Nakano, T.; Okamoto, Y. *Chem. Re*v. 2001, **101**, 4013-4038; (b) Oda, M.; Nothofer, H.-G.; Scherf, U.; Šunjic, V.; Richter, D.; Regenstein, W.; Neher, D. *Macromolecul*es 2002, **35**, 6792-6798; (c) Tian, G.; Lu, Y.; Novak, B. M. *J. Am. Chem. Soc.* 2004, **126**, 4082-4083.

(19) M. Szycher, *Szycher's handbook of polyurethanes*, 1999.

(20) O. Bayer, *Angewandte Chemie*, 1947, **59**, 257-272.

(21) R. B. Seymour and G. B. Kauffman, *J Chem Educ*, 1992, **69**, 909-910.

(22) Z. S. Petrovic and J. Ferguson, *Prog Polym Sci*, 1991, **16**, 695-836.

(23) D. Chattopadhyay and R. V. Kothapalli, *Prog Polym Sci*, 2007, **32**, 352–418.

(24) Z. Rafiee and V. Keshavarz, *Prog Org Coat*, 2015, **86**, 190-193.

(25) K. M. Zia, S. Anjum, M. Zuber, M. Mujahid and T. Jamil, *Int J Biol Macromol*, 2014, **66**, 26-32.

(26) C. Prisacariu, *Polyurethane elastomers: from morphology to mechanical aspects, Springer Science & Business Media*, 2011.
(27) G. Tersac, *Polymer International*, 2007, **56**, 820-820.
(28) S. A. Madbouly and J. U. *Otaigbe, Prog Polym Sci*, 2009, **34**, 1283-1332.
(29) T. Kochanė, S. Budrienė, K. Pielichowski and J. Pielichowski, *Chemija*, 2006, **17**, 74-89.
(30) J. Chen, J. Zhang, S.-H. Huang, Y.-X Wu, Z.-W. Bai, *Fenxi Kexue Xuebao* 2009, **25** (2), 161−165.
(31) P. G. Gudeangadi, T. Sakamoto, Y. Shichibu, K. Konishi and T. Nakano, *ACS Macro Lett.*, 2015, **4**, 901-906.
(32) M. M. Green, J. W. Park, T. Sato, A. Teramoto, S. Lifson, R. L. Selinger and J. V. Selinger, *Angew. Chem., Int. Ed.*, 1999, **38**, 3138–3154.

Chapter 2 . Synthesis, Structure, and Properties of Polyurethane Prepared from 1,4-Diisocyanatobenzene and 1,1'-Bi-2-naphthol at Various Enantiomeric Excesses

Introduction

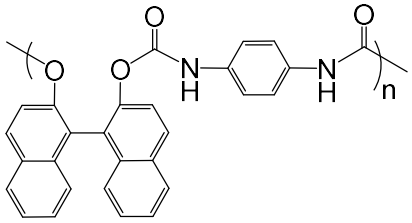

Poly(BINOL-*alt*-14DIB)

Chiral polymers are an important class of materials that find a wide variety of applications based on their chiral structures and properties.[1-10] Among various methods of chiral polymer synthesis, the most straightforward way is the polymerization of an optically active monomer where the chirality of the monomer is maintained in the resulting polymer structure and the polymer is therefore optically active. In such a polymerization, additional chiral conformation that is not present in the monomer structure may be induced through the polymerization. If a preferred-handed helical conformation is induced through the polymerization of an optically active monomer, the polymerization is not just a reaction connecting chiral units into a chain but is a helix-sense-selective polymerization (asymmetric helix-chirogenic polymerization).

As a novel example of helix induction through polymerization of optically active monomer, we recently introduced asymmetric polyaddition (copolymerization) of optically pure (*R*)-2,2'-dihydroxy-1,1'-binaphthyl ((*R*)-1,1'-bi(2-naphthol), BINOL) with 1,4-diisocyanatobenzene (14DIB) leading to a polyurethane.[11] The resulting polymer was proposed to adopt a left-handed 2/1-helical conformation which is based on the axial chirality of the BINOL units composing the chain (**Fig. 1**). Though polyurethanes are widely used in various polymeric materials,[12-15] the focus of polyurethane development is generally on novel chemical structures leading to new properties, and stereochemical

studies of polyurethanes are very rare.[16,17] In addition, an importance aspect involved in the finding of the helical polyurethane lies in the fact that this polymer had a helical conformation with a 2/1-pitch; such a helix is known for only limited polymers including this polyurethane, syndiotactic polystyrene, poly(*p*-methylstyrene), syndiotactic polypropylene, and syndiotactic polybutane in the solid state.[18-26] The helical conformation of poly(BINOL-*alt*-14DIB) is also characterized by a π-stacked conformation in which the aromatic groups comprising the main chain; this feature may open a way to use polymers for photo electronic applications.[27-30] WAXD profile of poly(BINOL-*alt*-14DIB) shows a diffraction peak at 2θ of 20.0 deg which supports that it has a π-stacked, 2/1-helical conformation with a stacking distance of 4.44 Å (**Fig. 2**). Further, the polymer does not show any clear melting point in differential scanning calorimetry (DSC) analysis which may mean that the 2/1-helical chains are not crystallized or packed in the solid state possibly due to the variation of chain lengths and supports that the diffraction peak is ascribed to intra-molecular π-stacking (**Figs. 3** and **4**).

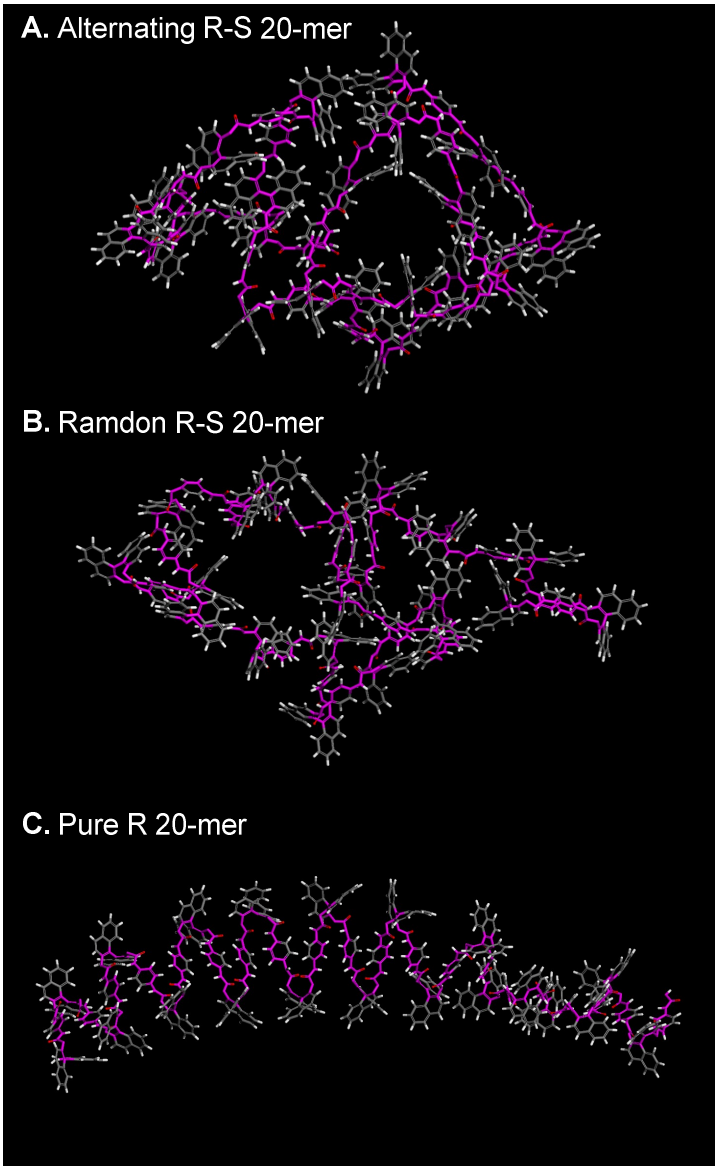

Fig. 1. Conformations of 20-mer chains of poly(BINOL-*alt*-14DIB) having alternating (R)-BINOL and (S)-BINOL units (a), randomly distributed (R)-BINOL and (S)-BINOL units (b) and only (R)-BINOL units obtained by MD simulations at 297K for 14-16 ns (NVT) using COMPASS force field. Total steric energies are 2826 kcal mol^{-1} (A), 2709 kcal mol^{-1} (B), and 2474 kcal mol^{-1} (C).

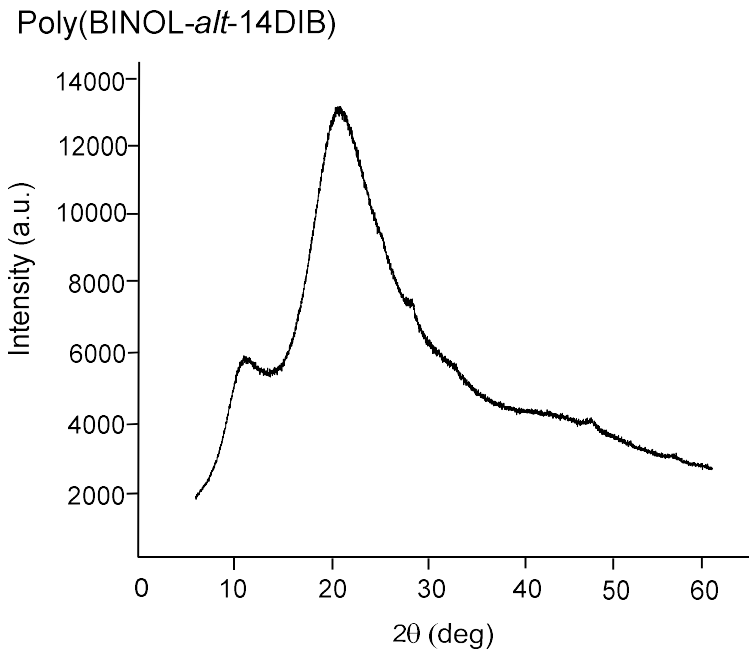

Fig. 2. WAXD profiles of poly(BINOL-*alt*-14DIB) (M_n 2720) [RIGAKU Miniflex diffractometer, CuKα, 30 KV, 10 mA, scan speed 1.25 degree/min, step 0.01 degree]

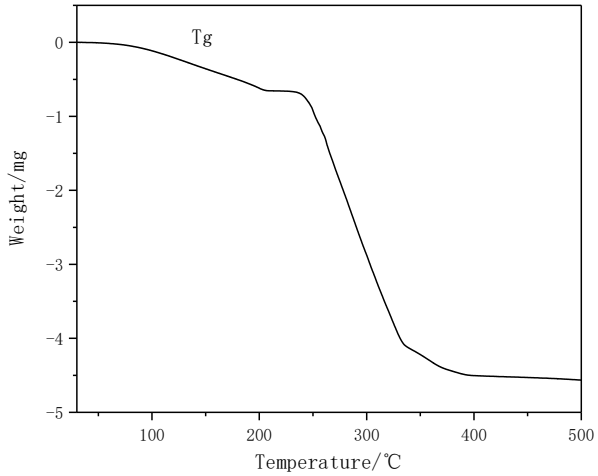

Fig. 3. Thermal gravimetric (TG) profiles of poly(BINOL-*alt*-14DIB) (M_n 2720) obtained at 100% e.e. of (*R*)-BINOL in feed [heating scan rate: 10 deg/min].

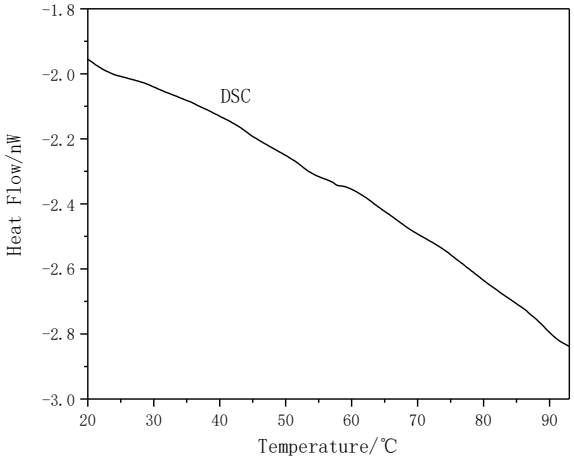

Fig. 4. DSC profiles of poly(BINOL-*alt*-14DIB) (M_n 2720) obtained at 100% e.e. of (*R*)-BINOL in feed [2nd heating scan at 10 deg/min].

Binaphthyl is an often-used chiral backbone which is effective in inducing a specific structure to polymer chain.[31-33] Although BINOL and its derivatives are known to racemized in excited states,[34,35] their chirality is robust and stable in the ground state; they are convenient building blocks of chiral polymeric structures.

In this work, polyurethanes were synthesized using 14DIB and BINOL having various enantiomeric excesses (e.e.'s), and the effects of chirality of BINOL on polymerization stereochemistry were investigated in detail (Scheme 1). Cyclic dimer was formed as well as linear polymer at all e.e.'s of BINOL, and the ratio of the cyclic dimer changed sensitively depending on e.e. of BINOL and was highest when racemic BINOL was used. The polymer chains were suggested to comprise of sequences with rather contiguous (*R*)-BINOL units rather than sequences with rather randomly distributed enantiomeric BINOL units.

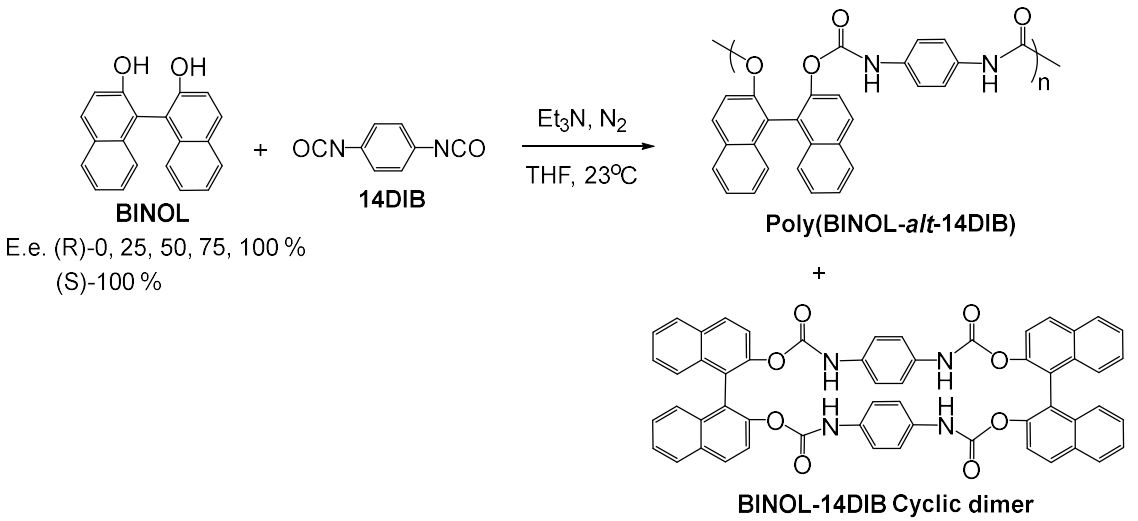

Scheme 1. Syntheses of polyurethanes and dimers from BINOL and 14DIB

Results and Discussion

The polymerization of 14DIB with (*R*)-BINOL at 0, 25, 50, 75, and 100 % e.e. or (S)-BINOL of 100% e.e. was conducted in tetrahydrofuran (THF) containing 5 % of Et_3N as a reaction promoter at [BINOL] = [14DIB] = 0.154 M at 23°C. At all e.e.'s BINOL was consumed at high conversion ratios. **Fig. 5** shows the size-exclusion chromatography (SEC) profiles of the reaction products obtained using (R)-BINOL monomers at different e.e.'s. All products contained significant amounts of cyclic dimer, and the dimer content was found to be higher at a lower e.e. of BINOL as estimated by wave-form analysis of the chromatograms (**Fig. 6**). The SEC curves also indicate that higher molar-mass products are formed in a higher yield at a higher e.e. of BINOL in feed.

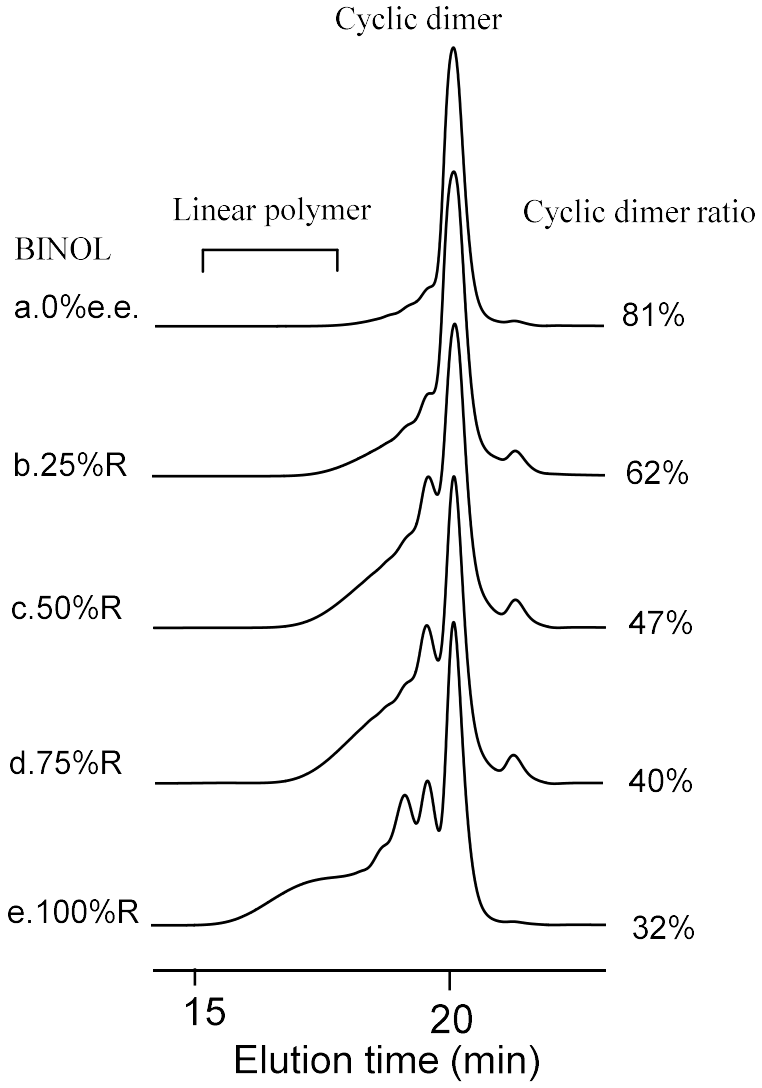

Fig. 5. SEC profiles of polymerization products obtained from 14DIB and (R)-BINOL at 0% e.e. (a), 25% e.e. (b), 50% e.e. (c), 75% e.e. (d), and 100% e.e. (e) with cyclic dimer contents estimated by wave-from analysis (Fig. 6) [detection by UV at 254 nm]

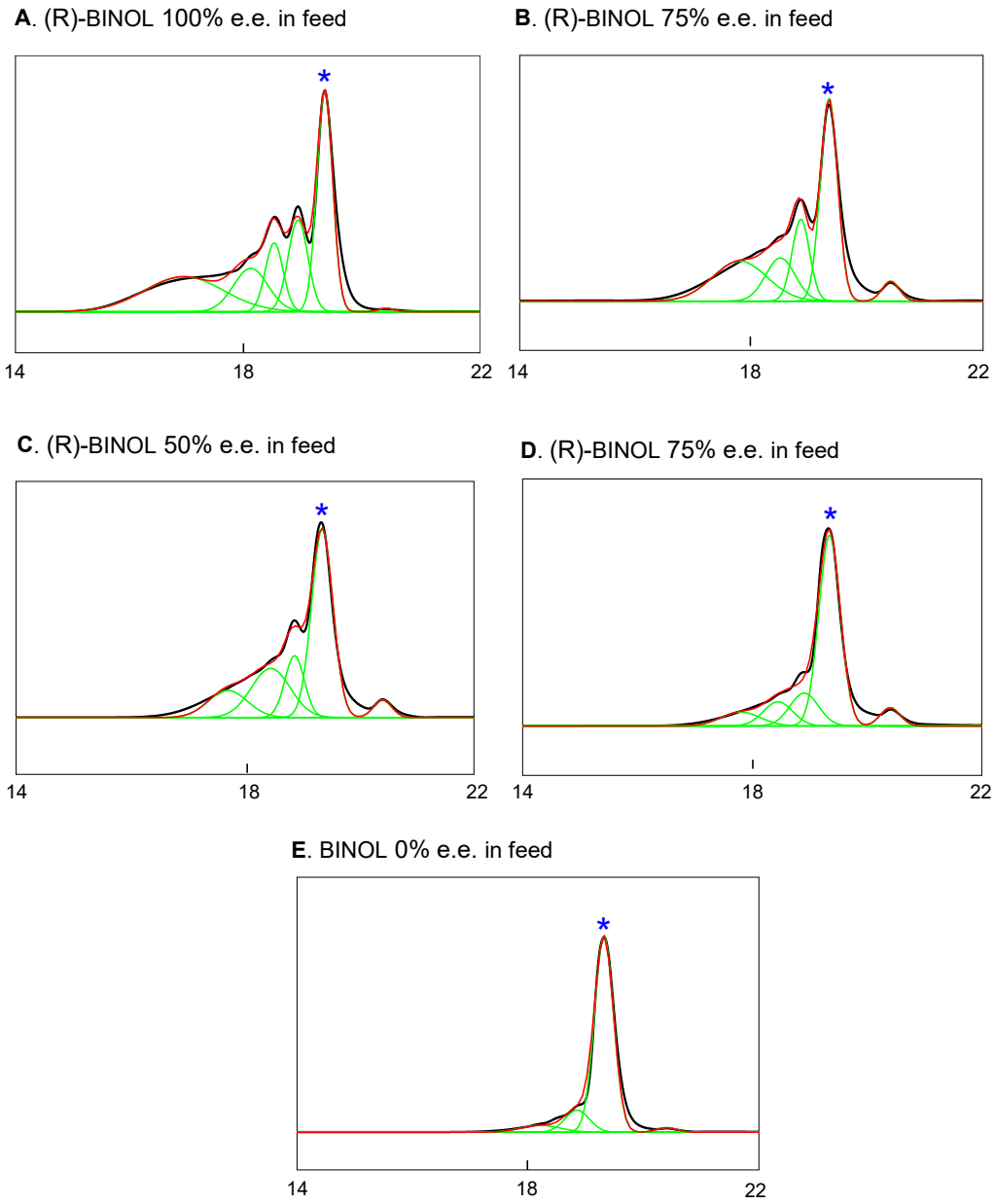

Fig. 6. Wave-form analysis of SEC curves of poly(BINOL-*alt*-14DIB) to determine the contents of cyclic dimer. Black curves are experimental SEC traces, green curves are deconvoluted Gaussian functions, and red curves are regenerated, entire SEC traces obtained by the addition of all deconvoluted functions. * denotes cyclic dimer peaks.

These results imply the following characteristics about monomeric sequences of polymer: (1) a random sequence of (R)- and (S)-BINOL units involving (R)-(S) junction does not grow to a longer chain, and (2) a longer chain tends to be composed of contiguous (R)-BINOL units. The former character is consistent with the fact that only a low-molar-mass polymer was produced in a low yield at 0% e.e. of BINOL in feed, and the latter character accounts for the fact that a higher-molar-mass polymer was produced in a higher yield at a higher e.e. of BINOL in feed. An actual polymer chain produced in the systems with (R)-BINOL in excess in feed would have a sequence structure composed of rather contiguous (R)-BINOL units as the majority component with sporadically incorporated, rather isolated (S)-BINOL units as the minority component. Production of chains consisting only of (R)-BINOL units and one consisting only of (S)-BINOL units at the same time may not be plausible even when racemic BINOL was used ("racemate-forming enantiomer-differentiating polymerization").

In connection with the sequence structure (distribution of enantiomeric BINOL units), three polymer models having different monomeric sequences were simulated by molecular dynamics and mechanics (MD and MM) calculations; the models are 20-mers composed of an alternating sequence of (R)- and (S)-BINOL units, composed of a random sequence of (R)- and (S)-BINOL units, and composed only of (R)-BINOL units having the proposed 2/1-helical conformation[11] (**Fig. 1**). The alternating and random chains have significantly different conformations from the 2/1-helix. In addition, the alternating and random chains had higher total steric energies (2826 kcal mol^{-1} and 2709 kcal mol^{-1}, respectively) than the proposed 2/1-helical structure (2474 kcal mol-1). These results support the conclusion based on the SEC curves that sequences composed of rather contiguous (R)-BINOL units would be preferred over random sequences.

When racemic BINOL was used, more than 80% of the products was the cyclic dimer. This observation may suggest that cyclic dimer tend to be composed of (R)- and (S)-BINOL molecules ((R,S)-dimer) rather than those composed of two (R)-BINOL molecules and two (S)-BINOL molecules ((R,R)-dimer and (S,S)-dimer). This aspect was assessed by HPLC separation of the three cyclic dimers (**Fig. 7**).

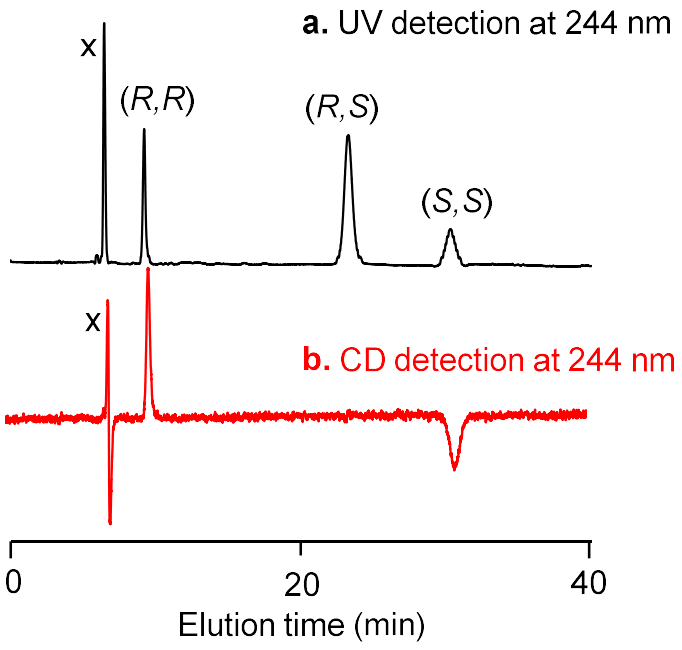

Fig. 7. HPLC separation/resolution of cyclic dimer obtained from racemic BINOL and 14DIB. x denotes solvent signals at void volume. [column = Chiralpak IA, eluent = CH_2Cl_2-hexane (95/5), flow rate 0.5 mL/min]

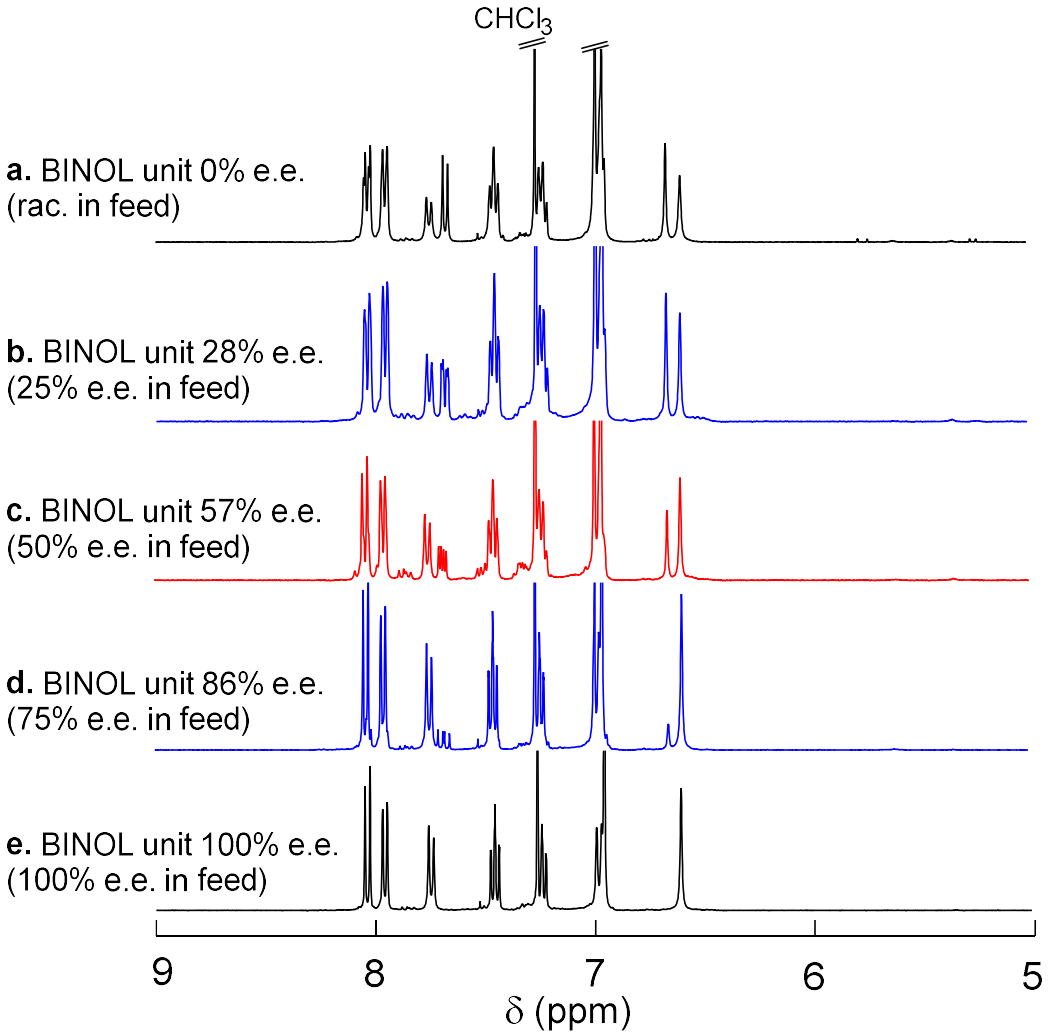

Fig. 8. ^{1}H NMR spectra of BINOL-14DIB cyclic dimers (mixtures of R-R, R-S, S-S dimers) having different e.e.'s of BINOL units prepared at different e.e.'s of BINOL in feed and isolated by preparative SEC: BINOL unit e.e. 0% (a), 28% (b), 57% (c), 86% (d), and 100% (e) (pure R-R cyclic dimer). [400 MHz, r.t., $CDCl_3$]

As shown in **Fig. 7**, clear, base-line separation/resolution by chiral HPLC was attained for the cyclic dimer under the chromatographic conditions noted in the figure legend. Among the three signals, the one at 23.3 min was assigned to (R,S)-cyclic dimer since this species did not show any CD detector responses. The absolute configurations of (R,R)- and (S,S)-cyclic dimers were assigned using the (R,R)-cyclic dimer sample

available from our recent work.[11] The accurate ratios of the three cyclic dimer species were determined by the HPLC analyses; the ratios are plotted against e.e. of BINOL in feed along with the theoretical (statistical) ratios of the three isomers calculated according to the ratios of (R)-BINOL to (S)-BINOL in feed (**Fig. 9**).

There is clear deviation of the observed ratios from the theoretical ratios; at 25%, 50%, and 75% e.e. of BINOL in feed, the ratio of (R,R)-isomer tends to be greater and that of (S,S)-isomer smaller than the corresponding theoretical values, suggesting that (R)-BINOL is incorporated into cyclic dimer more preferentially than expected from its concentration bias. Such preference could occur through autocatalysis[36,37] where (R,R)-isomer formed in the earlier stage of reaction might enhance the formation of the same species in the latter stages while the extent of preference is moderate, and the mechanism elucidation needs further studies.

On the other hand, in the reaction using racemic BINOL where there is no concentration bias on either enantiomer of BINOL, the ratio of (R,S)-cyclic dimer (60 %) is clearly higher than the corresponding theoretical value (50%). Under this condition, (R,S)-cyclic dimer was selected over (R,R)- and (S,S)-cyclic dimers in the reaction. This observation is in line with the conclusion about the monomeric sequence that a random sequence involving (R)-(S) junction does to grow to a high polymer; such the combination of (R)- and (S)-BINOL units tend to form a cyclic dimer.

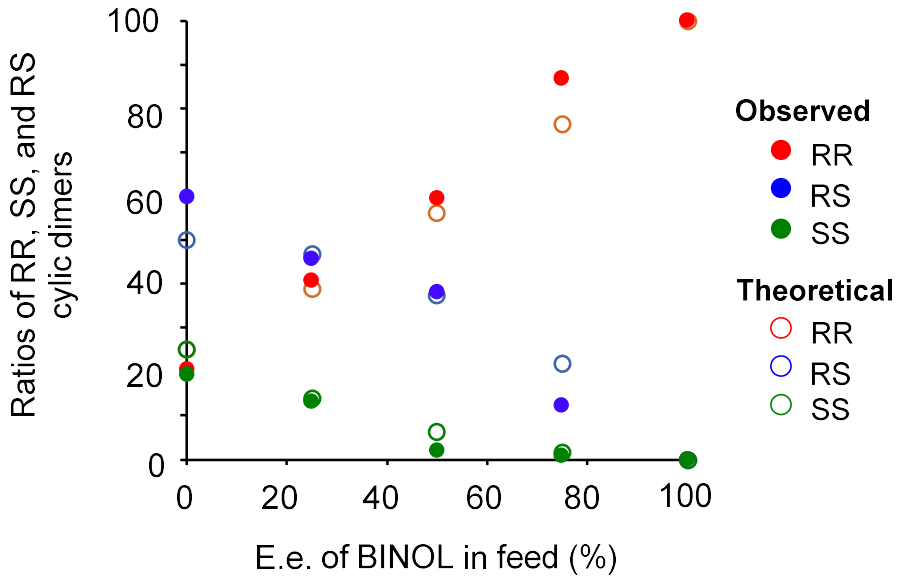

Fig. 9. Ratios of (R,R)-, (R,S)-, and (S,S)-cyclic dimers of BINOL and 14DIB plotted against e.e. of BINOL in feed: observed values [filled circles] and theoretical (statistical) values calculated based on e.e. of BINOL in feed [open circles].

With this result, a question may be whether or not (R,S)-cyclic dimer is substantially more stable over (R,R)- and (S,S)-cyclic dimers. In order to obtain information on this aspect as well as on the fact that cyclic dimers, not "linear dimers", are obtained, molecular dynamics and mechanics (MD and MM) calculations were conducted on cyclic dimers (**Fig. 10**).The total steric energies for (R,R)-cyclic dimer, (R,S)-cyclic dimer, (R,R)-linear dimer, and (R,S)-linear dimer were 409.5 kcal mol^{-1}, 390.69 $kcalmol^{-1}$, 288.56 $kcalmol^{-1}$, and 278.47 $kcalmol^{-1}$, respectively (COMPASS force field). (R,S)-cyclic dimer is indeed more stable than (R,R)-cyclic dimer, which may account for the preference of (R,S)-cyclic dimer over (R,R)-cyclic dimer in the racemic BINOL system. However, it is intriguing that the linear dimers are much more stable than the cyclic dimers in spite of the experimental fact that the cyclic dimers, not the linear dimers, are exclusively formed as dimers. Static energies of the dimes species hence cannot explain the formation cyclic dimers; they may be preferentially formed through kinetic control.

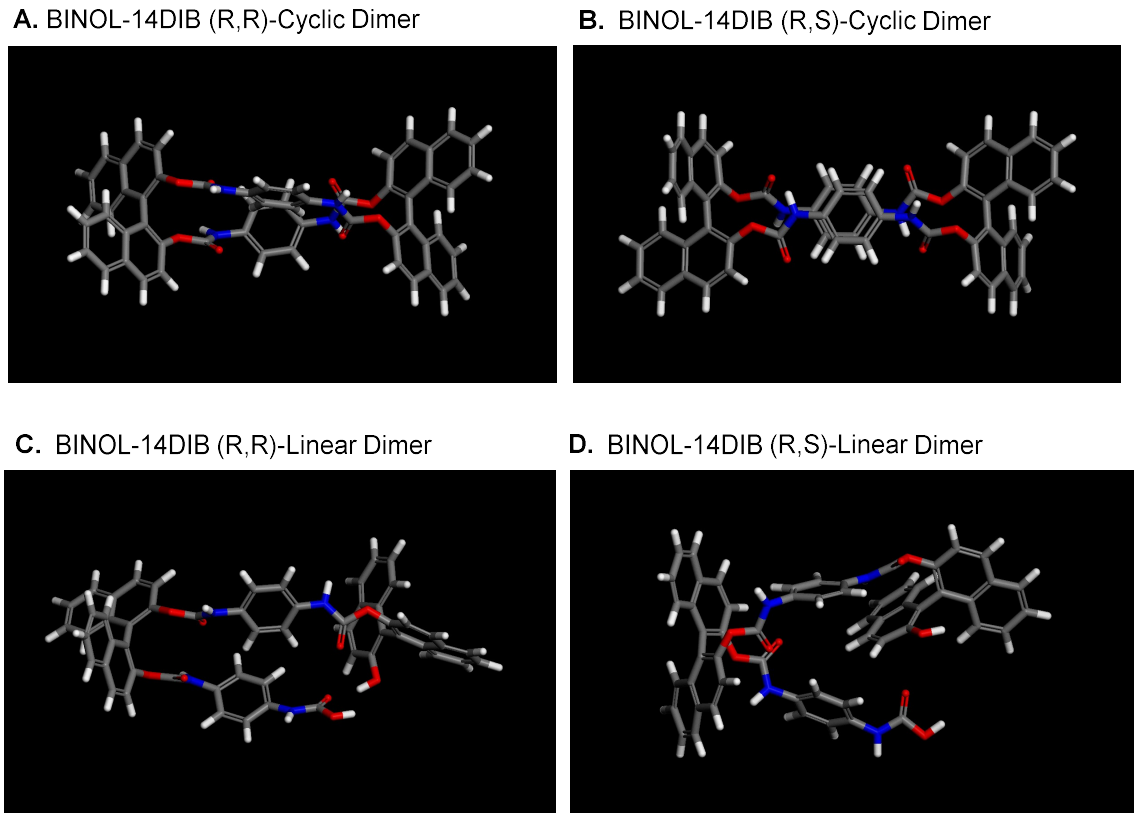

Fig. 10. Structures of (R,R)-cyclic dimer (A), (R,S)-cyclic dimer (B), (R,R)-linear dimer (C), and (R,S)-linear dimer (D) of the BINOL-14DIB system obtained by simulation. A and B were obtained through MM optimization of the corresponding crystal structures, and C and D were obtained by MD simulation for 3 nsec at 297K followed by MM optimization using COMPASS force field. Total steric energies are 409.5 kcal mol^{-1} (A), 390.69 $kcalmol^{-1}$ (b), 288.56 $kcalmol^{-1}$ (C), and 278.47 $kcalmol^{-1}$ (D).

The structure of (R,S)-dimer was unambiguously clarified by single crystal X-ray analysis where the presence of both (R)- and (S)-BNOL units connected to the central benzene rings through urethane bonds is clear (**Fig. 11**). The crystal was obtained by recrystallization from a mixture of $CHCl_3$, tetrahydrofuran, ethyl acetate and hexane; a $CHCl_3$ and a THF molecules are co-crystallized with the dimer. In the crystal, the two benzene rings are almost completely co-facially and closely π-stacked with a spacing

distance of ca. 3.8 Å. This structure is in a sharp contrast to that of the (R,R)-cyclic dimer already reported where the two benzene rings are arranged in a perpendicularly twisted manner.

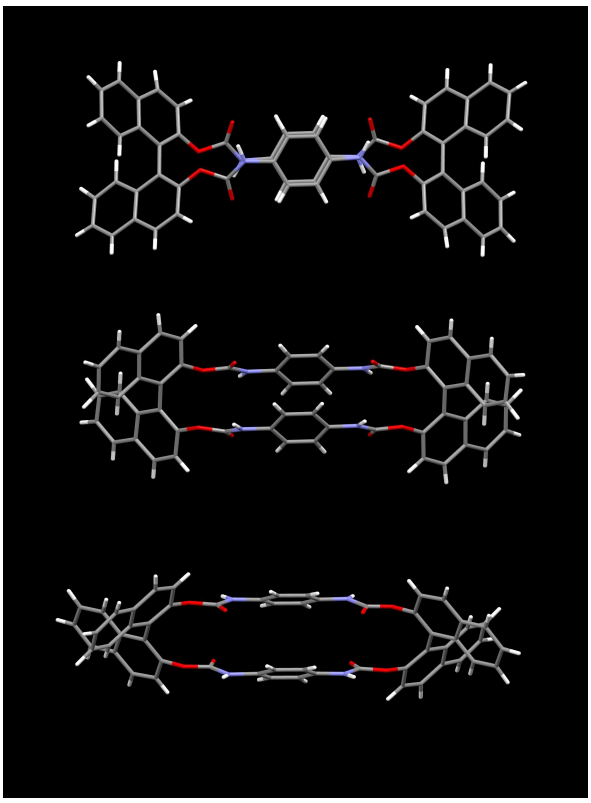

Fig. 11. Crystal structure of (R,S)-cyclic dimer obtained from *rac*-BINOL and 14DIB viewed from three different angles.

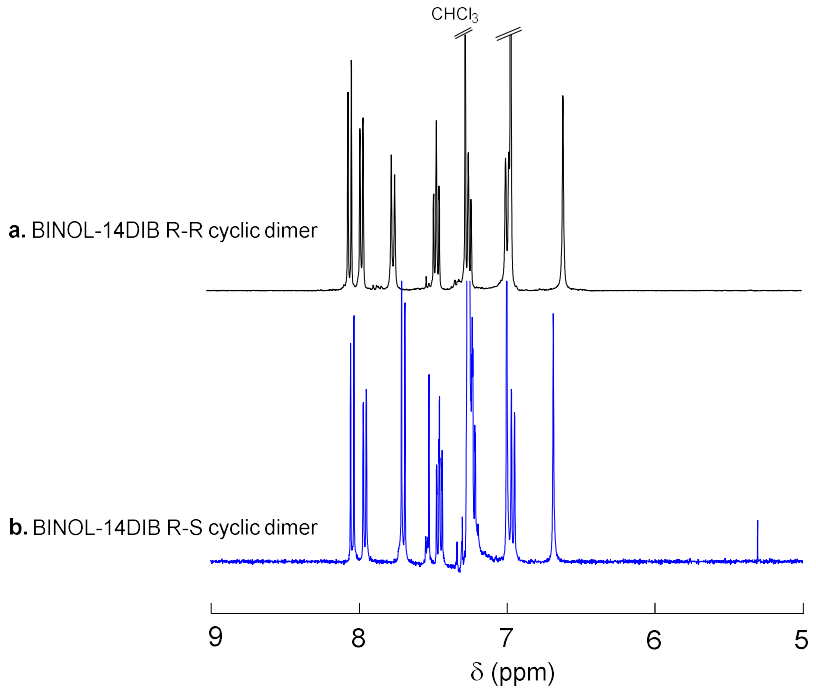

Fig. 12. ^{1}H NMR spectra of BINOL-14DIB cyclic dimers: pure R-R (a) and R-S cyclic dimers. [400 MHz, r.t., $CDCl_3$]

On the basis of the ratios of the three cyclic dimers and the contents of the cyclic dimers at different e.e. of BINOL, e.e.'s of BINOL units in polymers (all species excepting for the cyclic dimer in this context) as well as those of cyclic dimers were estimated and plotted against e.e. of BINOL in feed (**Fig. 13**). E.e.'s of BINOL units in cyclic dimer were slightly higher and those in polymer were slightly lower than the diagonal theoretical line connecting the data points at e.e. of BINOL in feed = 0% and 100%. These results may mean that (i) the cyclic dimers were formed prior to the linear polymers, (ii) (R)-BINOL was preferentially than incorporated into cyclic dimers where the extent of preference was more than expected from the concentration bias between the enantiomers, and (iii) the polymer was formed from the remaining BINOL having a lower e.e. that that in feed. In the BINOL-14DIB systems, chiral non-linear effects were thus observed in the selection of BINOL enantiomers. Chiral non-linear effects have been reported for

various polymer systems including polyisocyanates as representing examples of dynamic systems.[38]

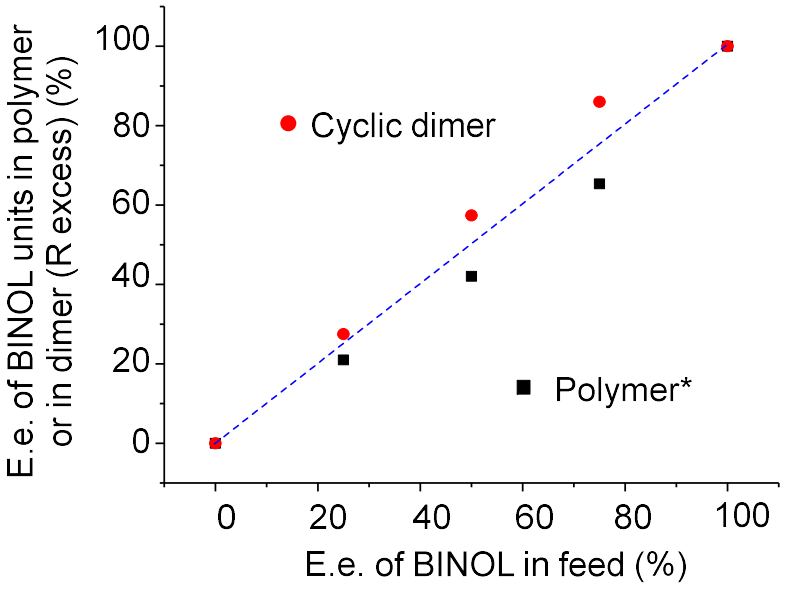

Fig. 13. E.e. of BINOL units in polymer and in cyclic dimer (R excess) plotted against e.e. of BINOL in feed. E.e. of units in polymer was calculated on the basis of e.e. in cyclic dimer and dimer content. *"Polymer" means all species excepting for the cyclic dimer.

In order obtain information on chiroptical properties of the polymers and dimers, CD and UV spectra of the samples prepared using (R)-BINOL at different e.e.'s and (S)-BINOL at 100% e.e. were measured in a THF solution and in a cast film (**Fig. 14**). The polymer samples were obtained by purification by preparative SEC, and had e.e.'s of BINOL units and following molar masses (vs. polystyrene): **a.** (S)-100% e.e., M_n 2960; **b.** (R)-21% e.e., M_n 2920 (25% e.e. of (R)-BINOL in feed), **c.** (R)-42% e.e., M_n 2740 (50% e.e. of (R)-BINOL in feed); **d.** (R)-65% e.e., M_n 2890 (75% e.e. of (R)-BINOL in feed); **e.** (R)-100%

e.e., M_n 3520. In a THF solution (**Fig. 14 A and B**), the polymers and dimers indicated intense Cotton splitting centered at 225 nm which is considered to be contributed mainly by the BINOL units; the (S)-BINOL-based polymer and cyclic dimer exhibited positive splitting and the (R)-BINOL-based polymers and cyclic dimers negative splitting, which accounts for the absolute chirality of BINOL units. On the other hand, the CD bands in the range of about 250-350 nm which may be contributed mainly by the -CO-NH-C_6H_4-NH-CO chromophore are considered to reflect helical chirality of the polymers and conformation of the cyclic dimers. This conclusion is supported by the fact that CD spectrum of BINOL in this range has a spectral pattern completely different from those of the polymers and dimers (**Fig. 15**).

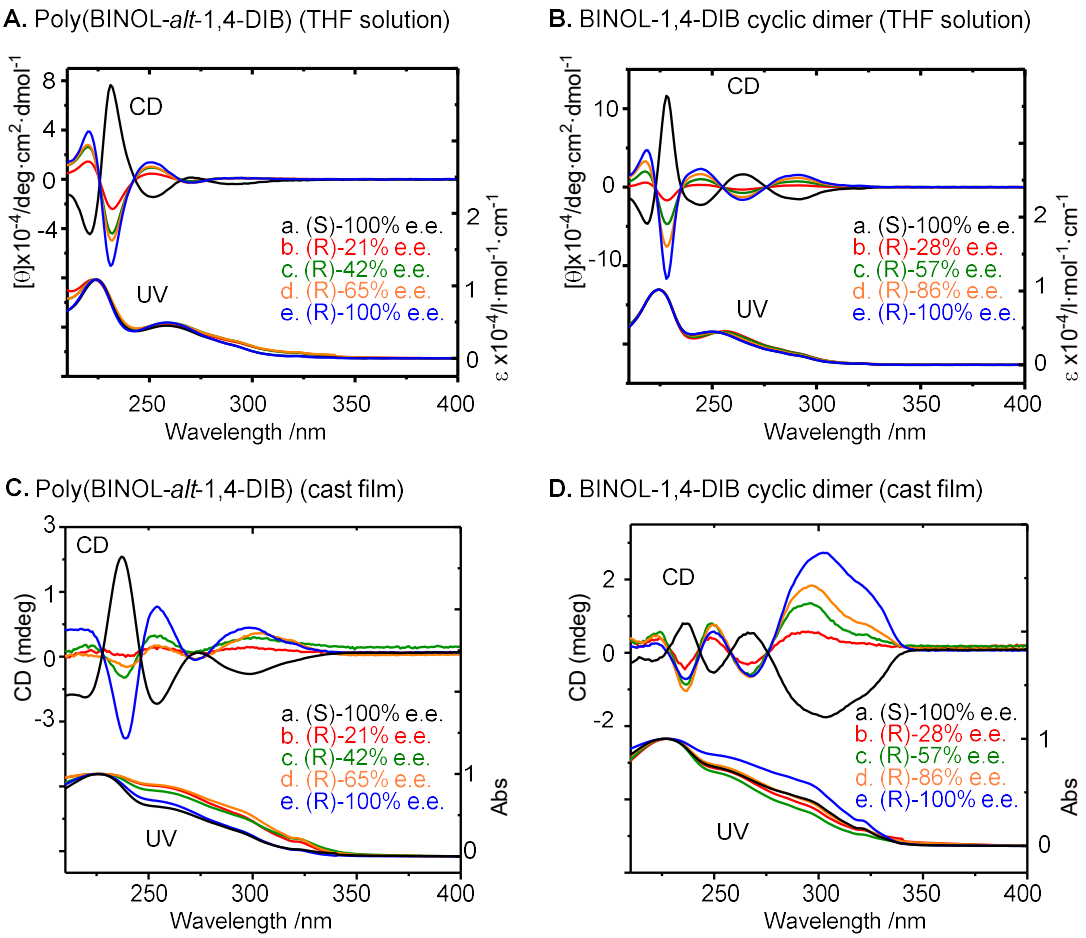

Fig. 14. UV and CD spectra of poly(BINOL-*alt*-14DIB) in THF (A) and in film (C) and those of cyclic dimer in THF (B) and in film (D). The solid-state spectra were obtained by averaging those recorded at four (90º interval) different film orientations (angles) with the film face positioned vertically to the incident light beam for measurement. The polymers samples were purified by preparative SEC and had following e.e.'s of BINOL units and molar masses (vs. polystyrene): **a.** (S)-100% e.e., M_n 2960; **b.** (R)-21% e.e., M_n 2920 (25% e.e. of (R)-BINOL in feed), **c.** (R)-42% e.e., M_n 2740 (50% e.e. of (R)-BINOL in feed); **d.** (R)-65% e.e., M_n 2860 (75% e.e. of (R)-BINOL in feed); **e.** (R)-100% e.e., M_n 3520. The polymers in b, c, and d in A contained a small amount of THF-insoluble part; concentrations of the solutions of these samples were normalized using the UV spectrum of a in A at 224 nm.

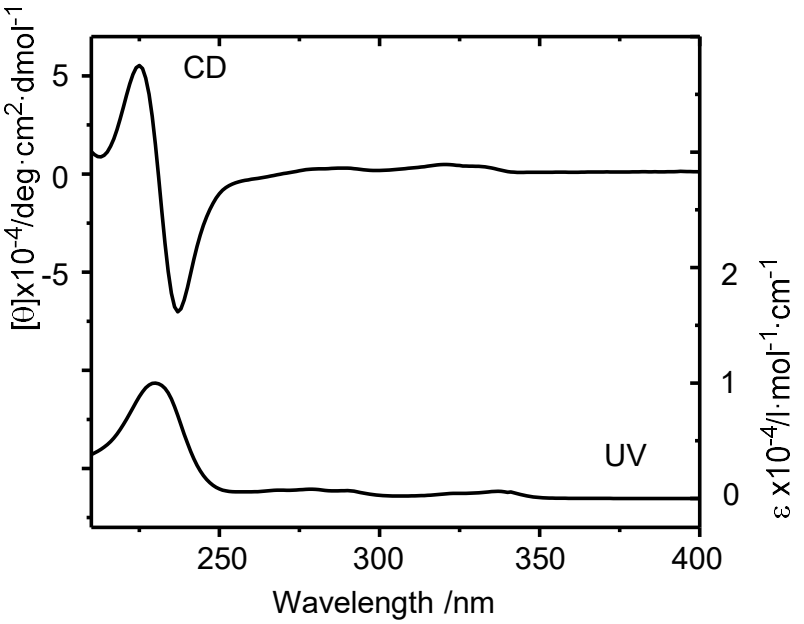

Fig. 15. CD and UV spectra of (R)-BINOL in THF.

The CD spectra of the cyclic dimers have more intense and clearer splitting bands in the range of 250-350 nm compared with the polymers which may reflect a twisted relative arrangement of the two CO-NH-C_6H_4-NH-CO chromophores connecting BINOL units leading to intra-chromophore exciton coupling effects. The distance the two CO-NH-C_6H_4-NH-CO chromophores is considered short enough to exert exciton coupling interactions.

In order to obtain further information from the CD spectra, the plots were made between relative CD intensity of the polymers and cyclic dimers obtained at different e.e.'s of BINOL in feed against e.e. of BINOL units in these species (**Fig. 16**). As for the polymers (**Fig. 16 A**), the relative CD intensity corresponding to BINOL units e.e. of 65, 42, and 21 % corresponding to the e.e. of 75%, 50%, and 25% of BINOL in feed were greater than expected from the linear, theoretical line connecting the data at 100% e.e. and 0% e.e., at all examined wavelengths (220, 231, 251, and 295 nm). Non-linearity was

especially remarkable for the CD band at 295 nm which mainly reflects helical chirality of the chain while it was moderate at the other wavelengths. The relative CD intensity at 295 nm seems to approach to the 100%-e.e. value even at a low e.e. of BINOL units while the deviation at the other three wavelengths are moderate. These results suggest that helical sense excess of the polymers is not proportional to e.e. of BINOL units, and a high helical sense excess is achieved even at a low e.e., implying that a sequence consisting of (S)-BINOL units as minority is forced to assume left-handed helicity due to chirality effects of a sequence consisting of contiguous (R)-BINOL units as majority through polymerization.

In a sharp contrast, the relative CD intensity for the cyclic dimers were only moderately lower than the values expected from the linear, theoretical line at all examined wavelengths (228, 244, 265, and 291 nm) and showed only slight non-linearity (**Fig. 16 B**). The moderate deviation from the theoretical could be attributed to intermolecular interactions among the three isomeric cyclic dimers though details of this aspect are not yet clear.

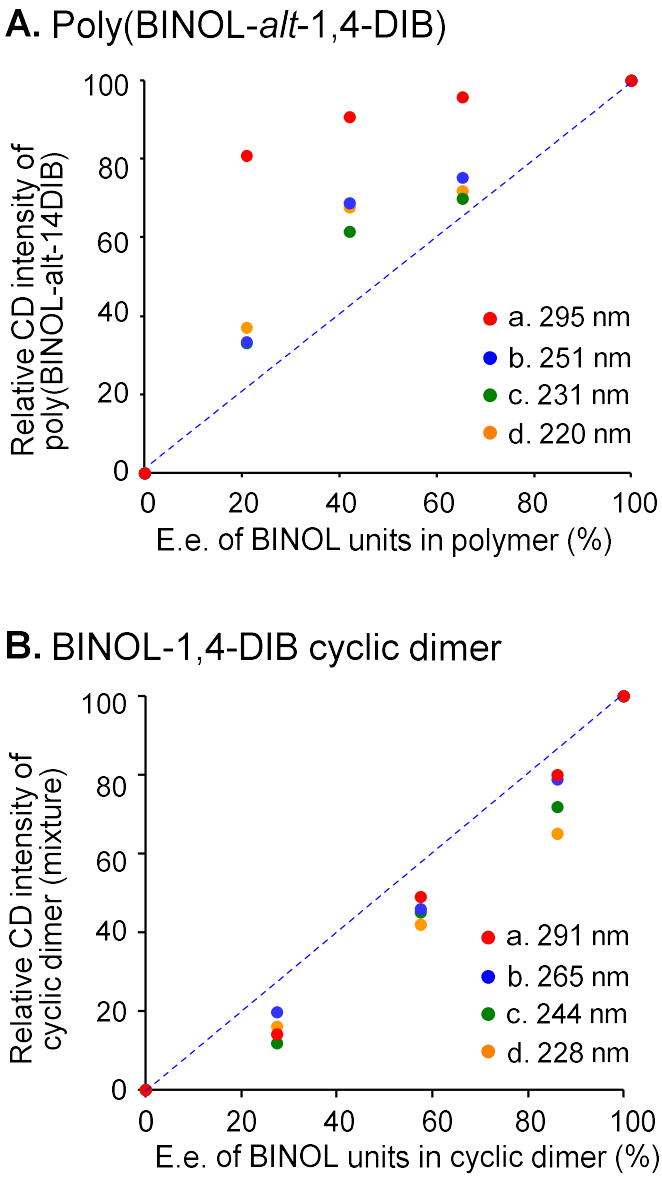

Fig. 16. Relation between relative CD intensities (absolute values of molar ellipticities) of poly(BINOL-*alt*-14DIB) in solution and e.e. of BINOL units in polymer at 310 nm (a), 251 nm (b), 231 nm (c), and 219 nm (d). In calculating relative CD intensities, molar ellipticities of the polymer and the cyclic dimer consisting only of (R)-BINOL units were set to 100.

Fig. 17 shows the ^{1}H NMR spectra of poly(BINOL-*alt*-14DIB) having different e.e.'s of BINOL units. All polymers exhibit rather broad signals which are consistent with the presence of rigid helical conformation. The up-field shifted aromatic signals in the range

of 6-7 ppm may be base on π-stacking of benzene-1,4-diyl moieties. Also, it can be confirmed that the relative intensities of the signals at around 7.8 ppm, 7.3, and 6.6 ppm those in the range of 5.6-6.2 ppm marked by downward arrows tended to decrease and the relative intensity of the signals at around 7.3 ppm marked by an upward arrow tended to increase with an increase in e.e. of BINOL units. These observations may be ascribed to the change in the ratio of (R)-BINOL units to (S)-BINOL units which are considered to be diastereomeric to each other in a left-handed helix. This is consistent with the aforementioned conclusion that the polymers have left-handed helical sense excess which is much higher than expected from e.e. of BINOL units due to non-linear chirality effects.

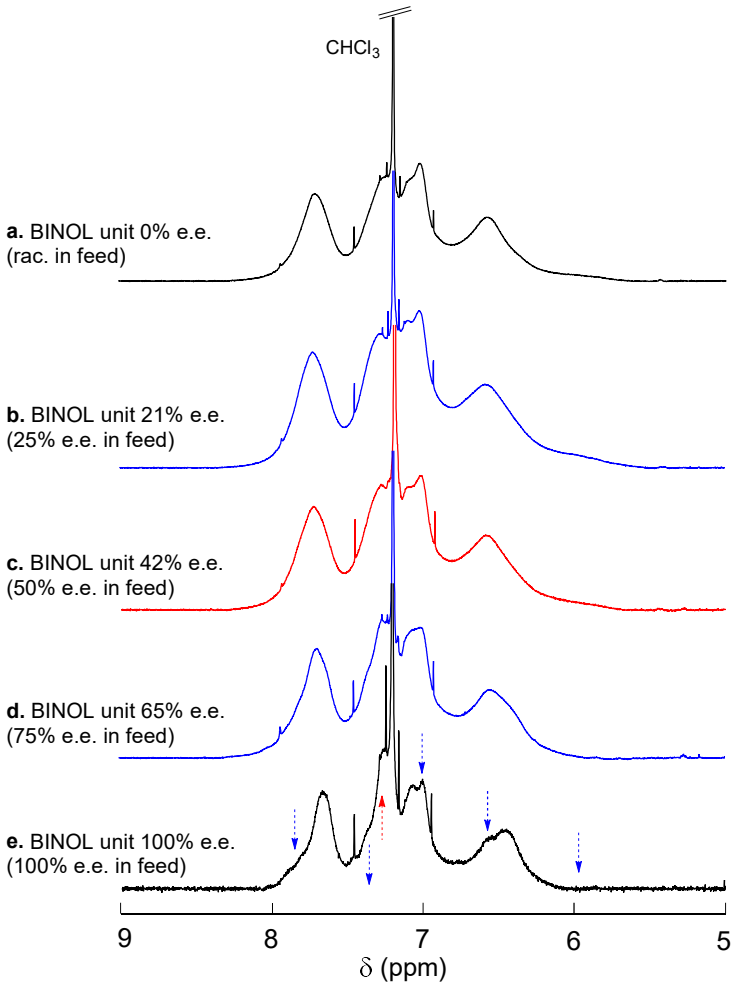

Fig. 17. ^{1}H NMR spectra of poly(BINOL-*alt*-14DIB)s having different e.e.'s of BINOL units: 0% (a), 21% (b), 42% (c), 65% (d), and 100% (e). [400 MHz, r.t., $CDCl_3$]

The polymers and cyclic dimers exhibited clearer CD spectra also in a cast film made from $CHCl_3$ solution than in solution (**Fig. 14 C and D**). The intensity of CD bands in the range of about 250-350 nm relative to those in the range of 200-250 nm was much higher in film than in solution, suggesting that chiral conformations of the polymers and cyclic dimers are stabilized and enhanced in the solid state. In order to take advantage of the chirality-enhanced helical structure of the linear polymers, circular polarized light

(CPL) emission measurements were attempted. Although the polymers exhibited an emission band centered at around 370 nm on phot excitation at 270 nm both in solution and film (**Fig. 18 and 19**)., they did not show any detectable CPL. Chirality of the polymers in excited states may not be significant even in the solid state.

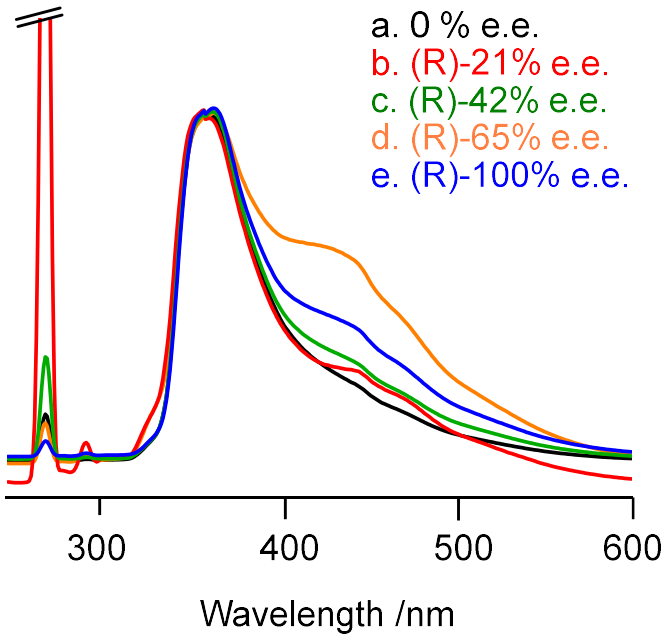

Fig. 18. Fluorescence spectra of poly(BINOL-*alt*-14DIB)s having different e.e.'s of BINOL units in a THF solution: **a.** (*R*)-21% e.e., M_n 2920 (25% e.e. of (*R*)-BINOL in feed), **b.** (*R*)-42% e.e., M_n 2740 (50% e.e. of (*R*)-BINOL in feed); **c.** (*R*)-65% e.e., M_n 2870 (75% e.e. of (*R*)-BINOL in feed); **d.** (*R*)-100% e.e., M_n 3520; **e.** (*R*)- 0% e.e., M_n 2320. [1-cm cell, conc. 1.0 x 10^{-3} M, λ_{ex} 270 nm]

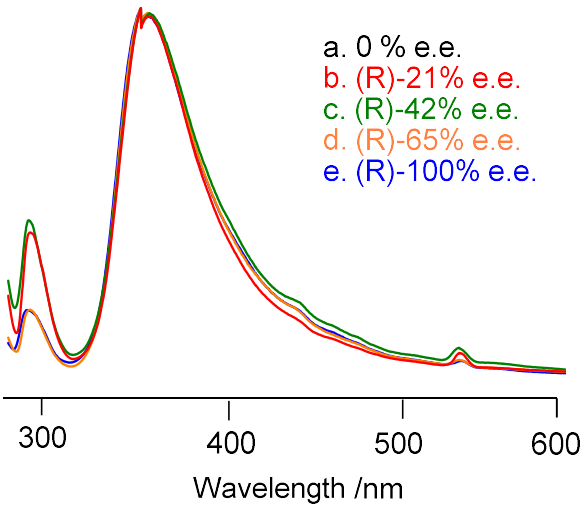

Fig. 19. Fluorescence spectra of poly(BINOL-*alt*-14DIB)s having different e.e.'s of BINOL units in a cast film: **a.** (*R*)-21% e.e., M_n 2920 (25% e.e. of (*R*)-BINOL in feed), **b.** (*R*)-42% e.e., M_n 2740 (50% e.e. of (*R*)-BINOL in feed); **c.** (*R*)-65% e.e., M_n 2870 (75% e.e. of (*R*)-BINOL in feed); **d.** (*R*)-100% e.e., M_n 3520; **e.** (*R*)- 0% e.e., M_n 2320.

Additional experiments were conducted to obtain information on the effects of molar mass and reaction time on UV and CD spectra of poly(BINOL-*alt*-14-DIB). As for the molar mass effects, three samples having M_n's of 2580, 1940, and 1540 were separated from the polymerization product obtained at 50% e.e. of BINOL in feed by preparative SEC showed very similar CD spectra and slightly different UV spectra (**Fig. 20**). These results may mean that the three samples have slightly different ratios of (R)- and (S)-BINOL units and imply that the enantiomeric BINOL monomers have different reactivities not only at the stage of cyclic dimer formation but also at the stage of polymer formation. As for the reaction time effects, samples obtained in 10 min and 24 h of polymerization at 50% e.e. of BINOL in feed showed very similar CD spectra and slightly different UV spectra (**Figs. 21** and **22**). **Fig. 21** shows that in both cases, BINOL

monomer was consumed at a high conversion ratio. The product obtained in 10 min consists mostly of the cyclic dimer while the one in 24 h contains a higher amount of polymer fractions, indicating that the cyclic dimer is formed first and then the polymer is formed by the intra-chain combination of shorter, linear chains (chain growth).

These results also appear consistent with the conclusion that enantiomeric BINOL monomers have different reactivities in the formation of polymer.

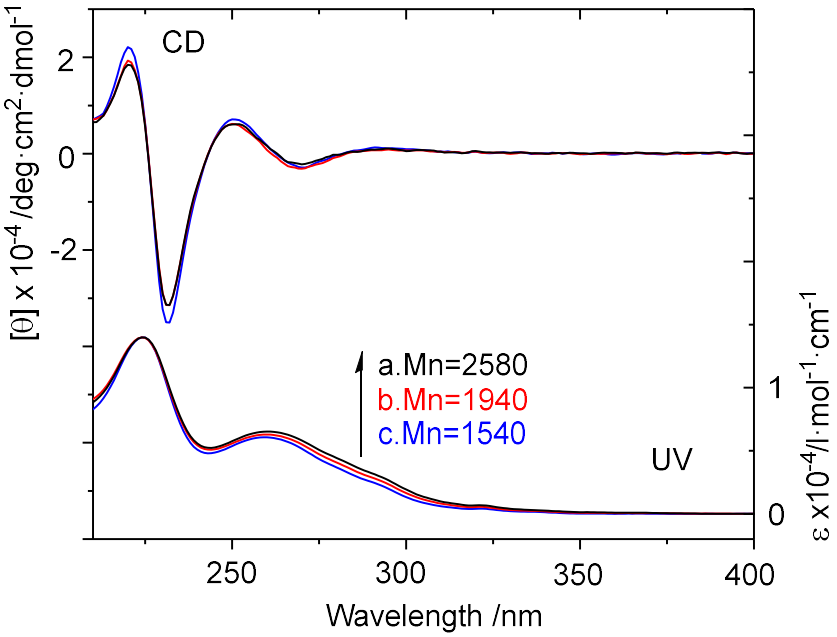

Fig. 20. UV and CD spectra of poly(BINOL-*alt*-14DIB)s of M_n 2580 (a), 1940 (b) and 1540 (c) obtained at 50% e.e. of (*R*)-BINOL in feed in THF solution. The samples were separated from the product of reaction at [BINOL] = [14DIB] = -0.154 M at room temperature for 24 h.

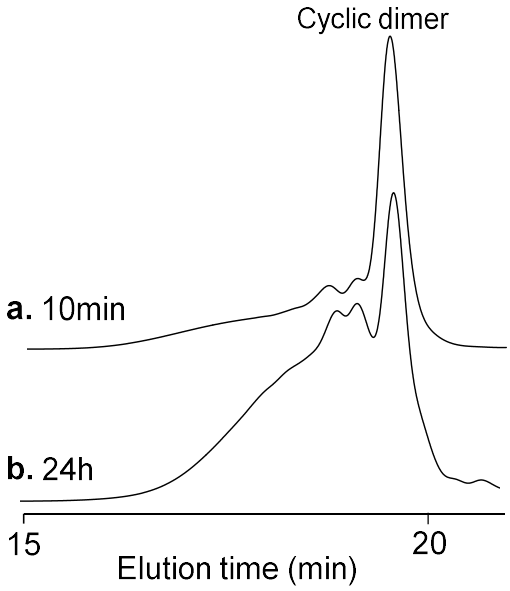

Fig. 21. SEC profiles of polymerization products obtained from 14DIB and (*R*)-BINOL at 50% e.e. in 10 min (A) and 24 h (B) of reaction at [BINOL] = [14DIB] = 0.154 M at room temperature. [detection by UV at 254 nm].

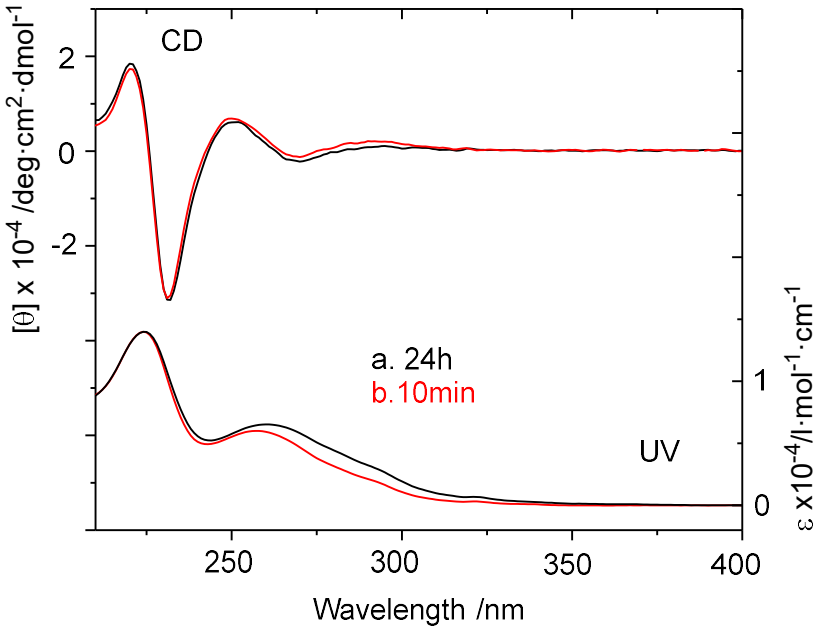

Fig. 22. UV and CD spectra of poly(BINOL-*alt*-14DIB)s obtained in 24 h (a) and 10 min (b) of polymerization at 50% e.e. of (*R*)-BINOL in feed in THF solution.

Conclusions

Polymerization behavior and properties and structure of products with a focus on stereochemistry were investigated in detail for BINOL-14DIB and BINOL-13DIB systems. In the BINOL-14DIB systems, cyclic dimers were formed along with helical, linear poly(BINOL-*alt*-14DIB) where the content of dimers was higher at a lower e.e. of BINOL and the yield of higher-molar-mass, linear polymers tended to be higher at a higher e.e. of BINOL in feed. The three forms of the cyclic dimer, i.e., (R,R)-, (R,S)-, and (S,S)-isomers, were completely resolved and separated by chiral HPLC, and their ratios were unambiguously determined. In the reaction using racemic BINOL, (R,S)-cyclic dimer was preferred over (R,R)- and (S,S)- cyclic dimers while (R,R)-cyclic dimer was preferred the other isomers when (R)-BINOL was present in excess over (S)-BINOL at 25-75% e.e. in feed; the latter observation might mean autocatalysis in the formation in (R,R)-cyclic dimer. As the cyclic dimers were found much less stable than the corresponding linear dimers by molecular simulations, the formation of the cyclic dimers may be based on kinetic control. Poly(BINOL-*alt*-14DIB) is proposed to compose of sequences with rather contiguous (R)-BINOL units as the majority component with rather sporadically incorporated (S)-units as the minor component. Helical sense excess appears to be greater than expected from the e.e. of BINOL units in the chain, suggesting that (S)-BINOL units sporadically incorporated in a rather contiguous (R)-BINOL units sequence become a part of left-handed helical conformation controlled by the chiral influence of (R)-BINOL units. These results may mean that, once a helix with one-handed helicity due to chirality of (R)-BINOL units is formed, the growing species may incorporate (S)-BINOL without changing helicity. Left-handedness of the chain is consistent with the absolute twist hand of (R)-BINOL with a negative dihedral angle, and it may be

reinforced by contiguous (R)-BINOL units. While the absolute twist hand of (S)-BINOL would favor right-handed helix, sporadically distributed or isolated (S)-units may not be effective in reversing the left-handed helical chain supported by contiguous (R)-BINOL units. Helicity of chains composed of enantiomeric monomeric units has been studied in detail for poly(3-methyl-1-pentene).[39,40]

Experimental

Materials. 1,4-Diisocyanatobeznene (TCI), (*R*)-(+)-1,1'-bi-2-naphthol (TCI), and (*S*)-(-)-1,1'-bi-2-naphthol (TCI) were used as purchased. Tetrahydrofuran (Kanto Chemical) was dried with sodium benzophenone ketyl and distilled immediately before use under N_2. Et_3N was distilled over CaH_2 and stored over KOH under nitrogen.

Synthesis of poly(BINOL-*alt*-14DIB). The synthetic procedure is described for the system with (*R*)-(+)-1,1'-bi-2-naphthol at 50% e.e. is described. To a solution of (*R*)-(+)-1,1'-bi-2-naphthol (0.1 g, 0.35 mmol) in THF (2 mL) were added 1,4-diisocyanatobenzene (0.056 mg, 0.35 mmol) and triethylamine (0.11 mL, 0.79 mmol) in this order under nitrogen atmosphere. The mixture was stirred for 24 h at room temperature and terminated by exposure to air. The polymer and cyclic dimer were isolated and purified by preparative SEC. SEC (vs. standard polystyrenes): M_n 2740, M_w/M_n 1.22. FT-IR (KBr) υ/cm^{-1}: 3405, 3062, 2962, 2923, 2852, 1726, 1610, 1512, 1261, 1191, 1096, 1077, 1033,1015, 803.

Film fabrication and annealing. Film samples were prepared from a $CHCl_3$ solution of a polymer by drop-casting on to a quartz plate (1 cm x 2 cm x 0.1 cm).

General instrumentation. ^{1}H NMR spectra were recorded on a JEOL JNM-ECX400 spectrometer (400 MHz for ^{1}H measurement) and a JEOL JNM-ECA600 spectrometer (600 MHz for ^{1}H measurement). SEC measurements were carried out using a chromatographic system consisting of a Hitachi L-7100 chromatographic pump, a Hitachi L-7420 UV detector (254 nm), and a Hitachi L-7490 RI detector equipped with TOSOH TSK gel G6000H_{HR} and G3000H_{HR} columns (30 x 0.72(i.d.) cm) connected in series (eluent THF, flow rate 1.0 mL/min). SEC analyses were also carried out at room temperature using a chromatographic system consisting of a JASCO PU-2080 PLUS intelligent HPLC pump, a JASCO UV-2075 PLUS intelligent UV/Vis detector (254 nm), a JASCO RI-930 intelligent RI detector, and a JASCO CO-1565 intelligent column oven (23 ºC) equipped with TOSOH TSK gel G6000H_{HR} and G3000H_{HR} columns (30 x 0.72(i.d.) cm) connected in series (eluent $CHCl_3$, flow rate 1.0 mL/min). Preparative SEC separation of dimers was performed using a JAI LC-908 preparative recycle chromatograph equipped with JAIGEL-1H and JAIGEL-2H columns connected in series (eluent $CHCl_3$). Chiral HPLC was performed using chromatographic system consisting of a JASCO DG-980-50 degasser, a JASCO PU-980 pump, a JASCO CD-2095plus CD detector, and a JASCO UV-2070plus UV detector equipped with a Daicel Chiral Pak IA

column (25 cm x 0.46 cm (i.d.)) [eluent CH_2Cl_2-hexane (95/1), flow rate 0.5 mL/min]. UV-vis absorption spectra were measured at room temperature with a JASCO V-550 and V-570 spectrophotometers. Steady-state emission spectra were taken on a JASCO FP-8500 fluorescence spectrophotometer. IR spectra were recorded on a JASCO FT/IR-6100 spectrometer using KBr pellet samples. Circular dichroism (CD) and linear dichroism (LD) spectra were taken with a JASCO-820 spectrometer. The spectra were obtained by averaging those recorded at four (90° interval) or two (180° interval) different film orientations (angles) with the film face positioned vertically to the incident light beam for measurement. Linear dichroism contributions were thus minimized to afford true CD spectra. Differential scanning calorimetry (DSC) and thermal gravity analysis (TGA) were taken on Rigaku Thermo Plus DSC8230 and TG8120 analyzer at a heating rate of 10 K/min in nitrogen atmosphere. WAXD measurement was performed on a RIGAKU Miniflex diffractometer.

Circularly polarized luminescence (CPL) emission measurements. Circularly polarized luminescence (CPL) measurements were attempted using a JASCO CPL-300 spectrophotometer for film samples.

Crystal structure analysis. Crystal data were collected on a Bruker SMART Apex II CCD diffractometer with graphite-monochromated Mo K_α radiation (λ = 0.71073 Å) at 90 K. The crystal structures were solved by direct methods (SHELXS-2013)[1] and refined by full-matrix least-squares methods on F^2 (SHELXL-2014)[2] with APEX II software. The carbon and oxygen atoms were refined anisotropically, and the hydrogen atoms were refined isotropically. Crystal data for *rac*-BINOL-14DIB cyclic dimer·2$CHCl_3$·2THF: $C_{66}H_{54}Cl_6N_4O_{10}$; M = 1275.83; 0.29 × 0.29 × 0.11 mm^3; monoclinic; space group $P2_1/c$ (no. 14); a = 10.8204(12) Å, b = 35.106(4) Å, c = 8.2849(9) Å; β = 110.005(1)°; V = 2957.2(6) $Å^3$; Z = 2; ρ_{calcd} = 1.433 gcm^{-3}; μ = 0.356 mm^{-1}; $2\theta_{max}$ = 50.06°; reflections collected: 14141, independent reflections: 5202 (R_{int} = 0.0456), $R_1(I>2\sigma)$ = 0.0500, $wR_2(I>2\sigma)$ = 0.1352; final difference map within +0.440 and -0.427 $eÅ^3$. CCDC-1952184 (*rac*-BINOL-14DIB cyclic dimer) contains the supplementary crystallographic data for this paper. These data can be obtained free of charge from The Cambridge Crystallographic Data Centre via www.ccdc.cam.ac.uk/data_request/cif.

Computational method. Wave-form analysis of SEC curves for determination of the contents of polymers and dimers were performed using Origin 2018 software package (Origin Lab). Molecular mechanics structure optimization was perfomed using the COMPASS force field implemented in the Discover module of the Material Studio 4.2

(Accelrys) software package with the Fletcher-Reeves conjugate gradient algorithm until the RMS residue went below 0.01 kcal/mol/Å. Molecular dynamic simulation was performed under a constant NVT condition in which the numbers of atoms, volume, and thermodynamic temperature were held constant. Berendsen's thermocouple was used for coupling to a thermal bath. The step time was 1 fs and the decay constant was 0.1 ps. Conformations obtained through MD simulation were saved in trajectory files at every 5 or 10 ps and were optimized by MM simulation.

References

(1) E. Yashima, N. Ousaka, D. Taura, K. Shimomura, T. Ikai and K. Maeda, *Chem. Rev.*, 2016, **116**, 13752-13990.

(2) E. Yashima, K. Maeda, H. Iida, Y. Furusho and K. Nagai, *Chem. Rev.*, 2009, **109**, 6102-6211.

(3) T. Nakano and Y. Okamoto, *Chem. Rev.*, 2001, **101**, 4013-4038.

(4) T. Nakano, *J. Chromatogr. A*, 2001, **906**, 205-225.

(5) Y. Okamoto and T. Nakano, *Chem. Rev.*, 1994, **94**, 349-372.

(6) J. Shen and Y. Okamoto, *Chem. Rev.*, 2015, **116**, 1094-1138.

(7) T. Nakano, *Chem. Rec.*, 2014, **14**, 369-385.

(8) R. Wang, Y. Zheng, X. Li, J. Chen, J. Cui, J. Zhang and X. Wan, *Polym. Chem.*, 2016, **7**, 3134-3144.

(9) Z. Yu, X. Wan, H. Zhang, X. Chen and Q. Zhou, *Chem. Commun.*, 2003, 974-975.

(10) J. Cui, J. Zhang and X. Wan, *Chem. Commun.*, 2012, **48**, 4341-4343.

(11) P. G. Gudeangadi, T. Sakamoto, Y. Shichibu, K. Konishi and T. Nakano, *ACS Macro Lett.*, 2015, **4**, 901-906.

(12) A. Caraculacu and S. Coseri, *Prog. in Polym. Sci.*, 2001, **26**, 799-851.

(13) E. Delebecq, J.-P. Pascault, B. Boutevin and F. Ganachaud, *Chem. Rev.*, 2013, **113**, 80-118.

(14) P. Krol, *Prog. Mater. Sci.*, 2007, **52**, 915-1015.

(15) D. A. Wicks and Z. W. Wicks Jr, *Pro. Org. Coat.*, 1999, **36**, 148-172.

(16) Y. Chen and J. J. Lin, *J. Polym. Sci. Part A: Polym. Chem.*, 1992, **30**, 2699-2707.

(17) T. Kobayashi, M.-a. Kakimoto and Y. Imai, *Polym. J.*, 1993, **25**, 969.

(18) Y. Chatani, Y. Shimane, T. Inagaki, T. Ijitsu, T. Yukinari and H. Shikuma,

Polymer, 1993, **34**, 1620-1624.

(19) C. De Rosa, P. Rizzo, O. de Ballesteros, V. Petraccone and G. Guerra, *Polymer*, 1999, **40**, 2103-2110.

(20) V. Petraccone, D. La Camera, B. Pirozzi, P. Rizzo and C. De Rosa, *Macromolecules*, 1998, **31**, 5830-5836.

(21) B. Pirozzi, R. Napolitano, G. Giusto and G. Ricci, *Macromol. Chem. Phys.*, 2008, **209**, 1012-1020.

(22) C. De Rosa and P. Corradini, *Macromolecules*, **1993**, *26*, 5711-5718.

(23) C. De Rosa and F. Auriemma, *Prog. Polym. Sci.*, **2006**, *31*, 145-237.

(24) C. D. Rosa, V. Venditto, G. Guerra and P. Corradini, Makromol. Chem., **1992**, *193*, 1351-1358.

(25) C. De Rosa, G. Guerra and A. Grassi, *Macromolecules*, **1996**, *29*, 471-472.

(26) C. De Rosa, F. Auriemma, L. Caliano, G. Talarico and M. Corradi, *Macromolecules*, **2008**, *41*, 5301-5306.

(27) T. Nakano and T. Yade, *J. Am. Chem. Soc.*, 2003, **125**, 15474-15484.

(28) T. Nakano, K. Takewaki, T. Yade and Y. Okamoto, *J. Am. Chem. Soc.*, 2001, **123**, 9182-9183.

(29) Y. Morisaki and Y. Chujo, *Angew. Chem. Int. Ed.*, 2006, **45**, 6430-6437.

(30) A. Cappelli, G. l. Pericot Mohr, M. Anzini, S. Vomero, A. Donati, M. Casolaro, R. Mendichi, G. Giorgi and F. Makovec, *J. Org. Chem.*, 2003, **68**, 9473-9476.

(31) Q.-S. Hu, D. Vitharana, G.-Y. Liu, V. Jain, M. W. Wagaman, L. Zhang, T. R. Lee and L. Pu, *Macromolecules*, 1996, **29**, 1082-1084.

(32) L. Pu, *Chem. Rev.*, 1998, **98**, 2405-2494.

(33) T. Takata, Y. Furusho, K.-i. Murakawa, T. Endo, H. Matsuoka, T. Hirasa, J.

Matsuo and M. Sisido, *J. Am. Chem. Soc.*, 1998, **120**, 4530-4531.

(34) Z. Zhang, Y. Wang and T. Nakano, *Molecules*, 2016, **21**, 1541.

(35) T. Hattori, Y. Shimazumi, O. Yamabe, E. Koshiishi and S. Miyano, *Chem. Commun.*, 2002, 2234-2235.

(36) K. Soai, T. Shibata, H. Morioka and K. Choji, *Nature*, 1995, **378**, 767.

(37) K. Soai, T. Shibata and I. Sato, *Acc. Chem. Res.*, 2000, **33**, 382-390.

(38) M. M. Green, J. W. Park, T. Sato, A. Teramoto, S. Lifson, R. L. Selinger and J. V. Selinger, *Angew. Chem. Int. Ed.*, 1999, **38**, 3138-3154.

(39) C. De Rosa, C. Santillo, R. Di Girolamo, G. Leone and G. Ricci, *CrystEngComm*, **2015**, 17, 6006-6013.

(40) C. De Rosa, F. Auriemma, C. Santillo, R. Di Girolamo, G. Leone, A. C. Boccia and G. Ricci, *Macromolecules*, **2015**, *48*, 5251-5266.

Chapter 3. Synthesis, Structure, and Properties of Polyurethane Prepared from 1,3-diisocyanatobenzene and 1,1'-Bi-2-naphthol at Various Enantiomeric Excesses

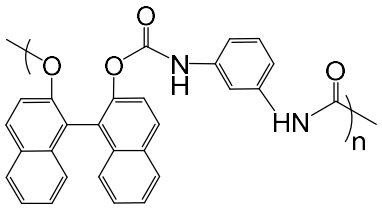

Poly(BINOL-*alt*-13DIB)

Polyurethane is an important class of polymers used for various applications.[1-10] As discussed in Chapter 2, chiral polyurethanes prepared from BINOL at various e.e.'s with 1,4-diisocynanatobenzene (14DIB) showed rich stereochemical aspects including non-linearity in helix induction where the majority enantiomer of BINOL controls the helicity and the minority enantiomer becomes a part of the helical sense which the minority enantiomer itself would not prefer. In this chapter, polyurethanes prepared by polyaddition of BINOL at various e.e.'s with 1,3-diisocynanatobenzene (13DIB) (Scheme 1) will be discussed. 13DIB and 14DIB are different only in the substitution positions of the two isocyanite groups. However, we observed significant differences between the reactions leading to poly(BINOL-*alt*-13DIB) and poly(BINOL-*alt*-14DIB) and also in the stereostructure of the two polymers. It is quite interesting that the subtle difference in the structure of DIB leads to such differences in polymer stereochemistry. Poly(BINOL-*alt*-13DIB) was suggested to possess a helical conformation which is distinguished from that of poly(BINOL-*alt*-14DIB) in the shape and in chiroptical properties. In the systems with 13DIB, the production of cyclic dimer was not confirmed, while linear dimer was identified as major oligomeric species.

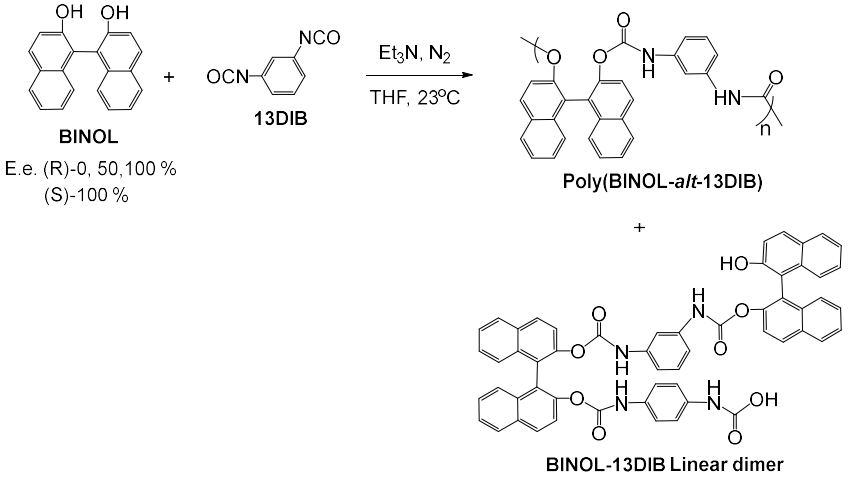

Scheme 1. Syntheses of polyurethanes and dimers from BINOL and 13DIB

Results and Discussion

Synthesis, structure and properties of poly(BINOL-*alt*-13DIB)

Poly(BINOL-*alt*-13DIB)s were prepared from racemic BINOL and (R)-BINOL at 50% and 100% e.e. with 13DIB in the same manner applied for the poly(BINOL-*alt*-14DIB) synthesis. The subtle difference in the substitution position of the diisocyanate monomers remarkably was found to significantly alter the polymerization behavior and the product structure. The polymerization was conducted in in THF containing 5 % of Et_3N at [BINOL] = [13DIB] = 0.154 M at 23°C, and the monomers were almost completely consumed. **Fig. 23** shows the SEC curves the polymerization products obtained at different e.e.'s of BINOL in feed. In a sharp contrast to the polymerization systems with 14DIB, the shapes of SEC curves were very similar to each other regardless and the ratio of the largest peak which is assigned to a "linear dimer" as discussed later was almost constant regardless of e.e. of BINOL in feed. Although it is difficult to assume a sequence structure of poly(BINOL-*alt*-13DIB), ^{1}H NMR spectra lead to relevant

information.

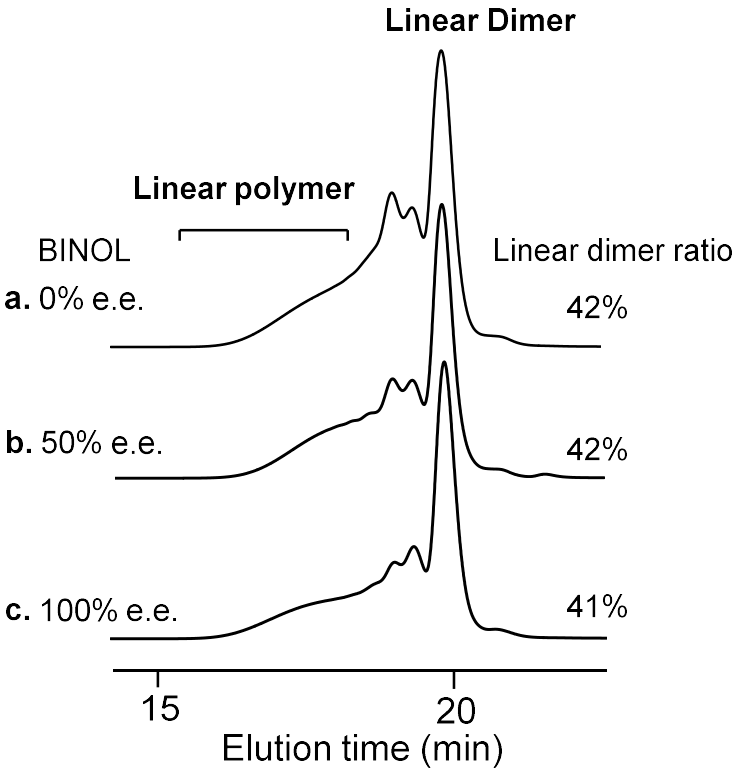

Fig. 23. SEC profiles of polymerization products obtained from 13DIB and (R)-BINOL at 0% e.e. (a), 50% e.e. (b), and 100% e.e. (c) associated with linear dimer contents estimated by wave-from analysis by wave-form analyses (Fig. 24). [detection by UV at 254 nm]

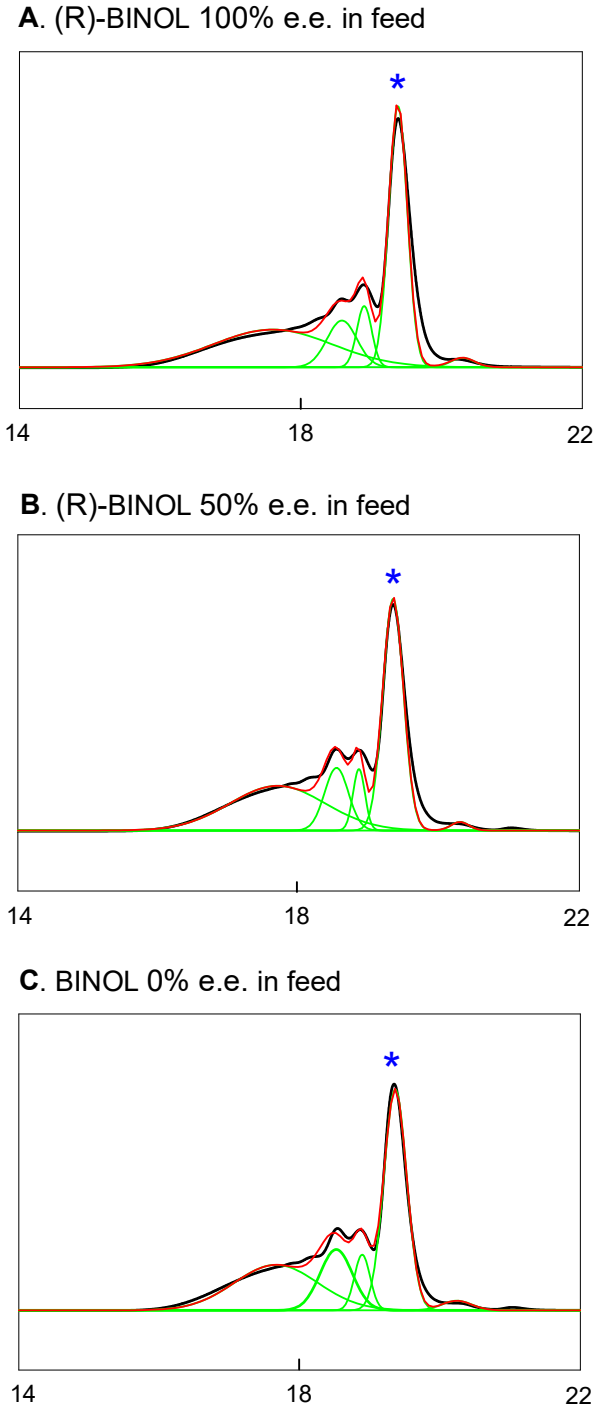

Fig. 24. Wave-form analysis of SEC curves of poly(BINOL-*alt*-13DIB) to determine the contents of linear dimer. Black curves are experimental SEC traces, green curves are deconvoluted Gaussian functions, and red curves are regenerated, entire SEC traces obtained by the addition of all deconvoluted functions. * denotes linear dimer peaks.

Fig. 25 shows the ^{1}H NMR spectra of the poly(BINOL-*alt*-13DIB)s obtained at different e.e's of BINOL. The spectral shape varied depending on 100% e.e. of BINOL in feed where the relative intensity of the signal at 7.7 ppm marked by upward arrows increased and those at around 7.1 ppm and in the range of 5.2-6.8 ppm marked by downward arrows decreased with an increase in e.e. of BINOL unit in feed. The fact that the spectral shapes of the polymers obtained from racemic BINOL and pure (R)-BINOL are remarkably different rules out independent formation of a chain comprised purely of (R)-BINOL units and one comprised of (S)-BINOL units which would be mirror images having opposite helical senses ("racemate-forming enantiomer-differentiating polymerization") in the system with racemic BINOL. The former chain is formed in the system with pure (R)-BINOL in feed. Sequences comprising of rather randomly distributed (R)-BINOL and (S)-BINOL units may be more plausible for the actual polymer chains; the two units would be diastereomeric to each other in a single-handed helical chain and can show different positions of signals. Production of rather random chains is also in line with the result that SEC profiles were almost unchanged regardless of e.e. of BINOL in feed.

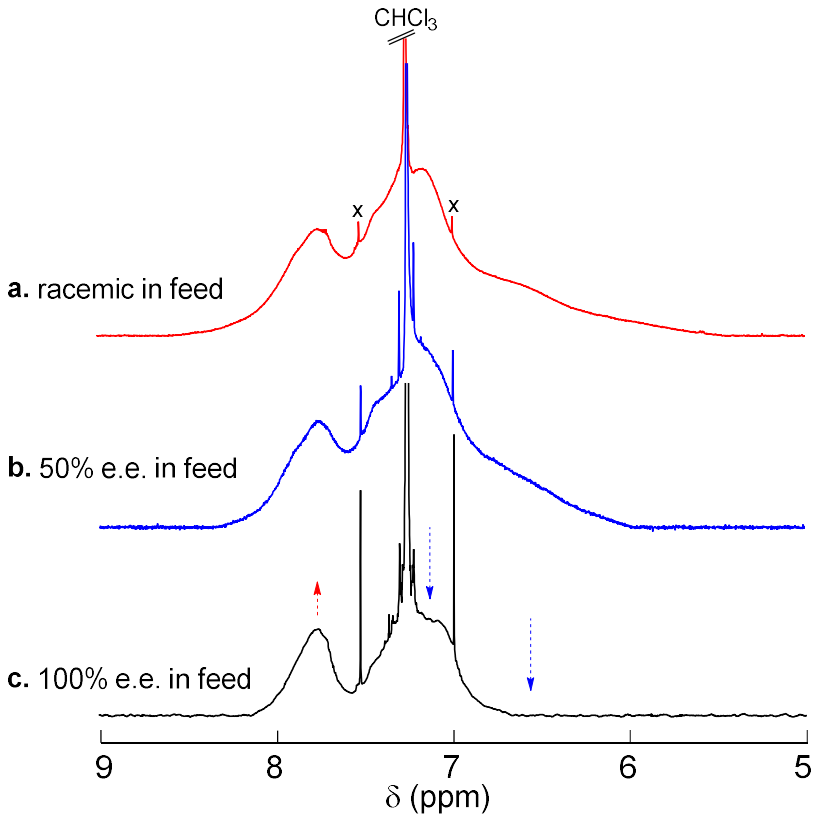

Fig. 25. ^{1}H NMR spectra of poly(BINOL-*alt*-13DIB)s obtained at different e.e.'s of BINOL in feed: 100% (M_n 2840) (a), 50% (M_n 3430) (b), and 0% (M_n 3270) (c). [400 MHz, r.t., $CDCl_3$]

It is noteworthy that poly(BINOL-*alt*-13DIB) made from (R)-BINOL at 100% e.e. lacks the signals in the range of 6-7 ppm while poly(BINOL-*alt*-14DIB) has signals in this range due to π-stacking. This observation suggests that conformation of poly((R)-BINOL-*alt*-13DIB) differs from that of poly((R)-BINOL-*alt*-14DIB), left-handed 2/1-helical structure with π-stacking character.

The structure of the dimer was assessed by preparative SEC fractionation from the product mixtures obtained at 50% and 100% e.e. of BINOL in feed and ESI-mass and ^{1}H NMR analyses (**Fig. 26**). The fractionated dimer sample showed a molar mass of 910.29

corresponding to the "linear dimer" (**Scheme 2**, exact mass: 910.40), supporting that this species is a dimer having a linear chain structure, not a cyclic structure. The 1,3-substitution pattern of the benzene of 13DIB ring may make the ring closure difficult.

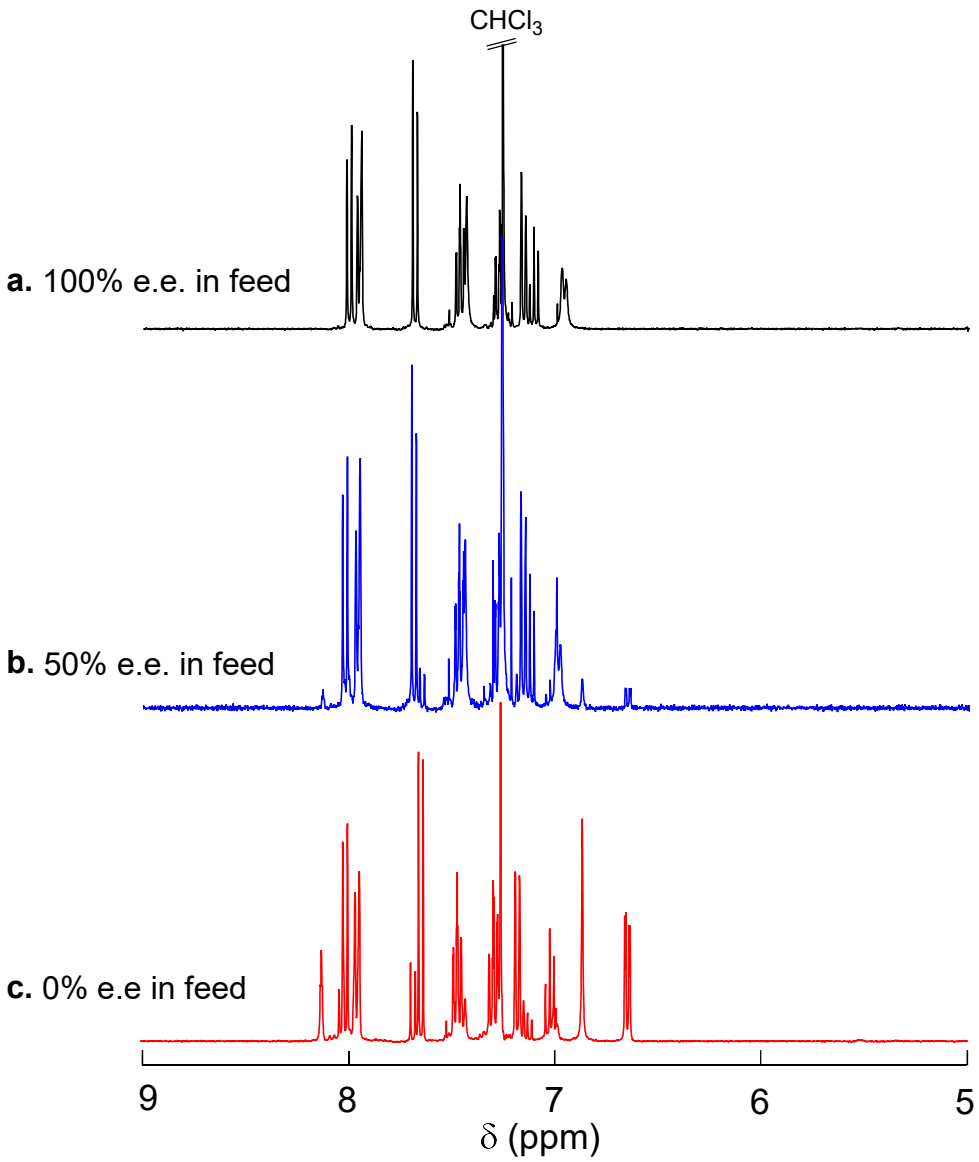

Fig. 26. ^{1}H NMR spectra of BINOL-13DIB linear dimers isolated by preparative SEC from the products at different e.e.'s of BINOL in feed: e.e. in feed 0% (a), 50% (b), and 100% (c). [400 MHz, r.t., $CDCl_3$]

Molecular dynamics and mechanics (MD and MM) calculations were conducted for the

linear dimers and hypothetical cyclic dimers in the same way as applied for the dimers in the BINOL-14DIB systems (**Fig. 27**). The linear dimers having (R,R)- and (R,S)-configurations had total steric energies of 262.3 kcal mol^{-1} and 279.0 kcal mol^{-1}, respectively, and the cyclic dimers having (R,R)- and (R,S)-configurations 381.9 kcal mol^{-1} and 396.1 kcal mol^{-1}, respectively. The cyclic dimers were found to be much less stable than the linear dimers probably due to ring strain, which would explain the production of the linear dimers in the BINOL-13DIB systems. The tendency that linear dimers are more stable than cyclic dimers in simulations is common between the BINOL-14DIB systems and the BINOL-13DIB systems while the former led to the cyclic and the latter the linear dimers. Kinetic control over the reactions might have different magnitudes in the two systems.

A. BINOL-13DIB (R,R)-Cyclic Dimer

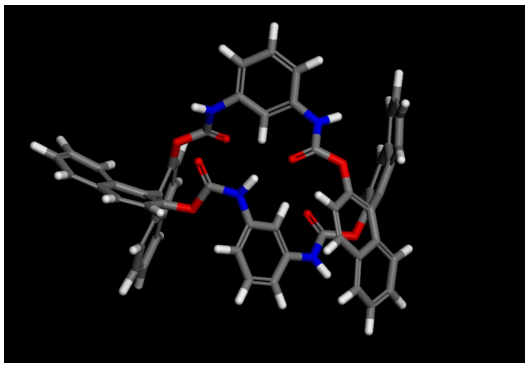

B. BINOL-13DIB (R,S)-Cyclic Dimer

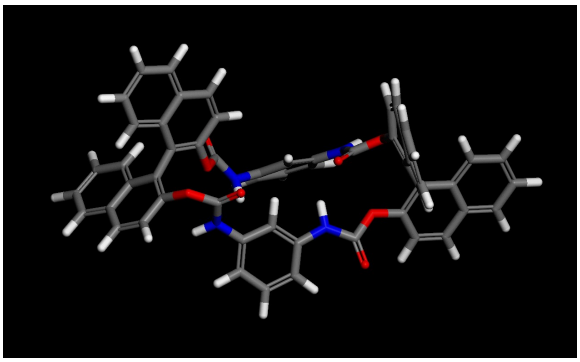

C. BINOL-13DIB (R,R)-Linear Dimer

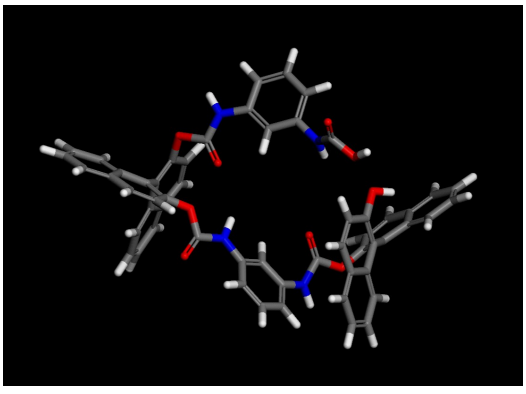

D. BINOL-13DIB (R,S)-Linear Dimer

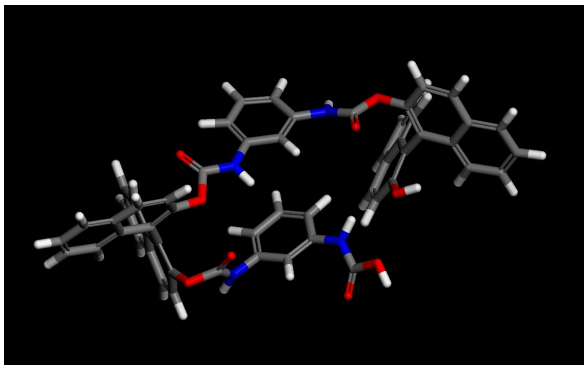

Fig. 27. Structures of (R,R)-cyclic dimer (A), (R,S)-cyclic dimer (B), (R,R)-linear dimer (C), and (R,S)-linear dimer (D) of the BINOL-13DIB system obtained by MD simulation for 3 nsec at 297K followed by MM optimization using COMPASS force field. Total steric energies are 381.9 kcal mol^{-1} (A), 396.1 kcal mol^{-1} (B), 262.3 kcal mol^{-1} (C), and 279.0 kcal mol^{-1} (D).

Unlike the BINOL-14DIB cyclic dimers, the BINOL-13DIB linear dimers were not able to be separated by chiral HPLC and the isomeric ratios are hence not known. The CD/UV spectra of the linear dimers obtained at 50% and 100% of BINOL are shown in **Fig. 28 A**. The CD spectra of the dimers have very similar shapes to each other, and the spectral intensities are closer than expected from the difference in e.e. of BINOL in feed. These results suggest two possibilities, *i.e.*, (i) BINOL unit isomeric ratios are similar in the two linear dimers ((R)-isomer was highly preferred in the formation of linear dimer at 50% of BINOL in feed), or (ii) the CD spectra mainly reflect conformational chirality of linear dimer and the dimer obtained at 50% of (R)-BINOL in feed has a conformation similar to that obtained at 100% of (R)-BINOL in feed. The latter might be more plausible because very high selectivity of enantiomer was not observed in the BINOL-14DIB systems. The fact that the linear dimers' spectral shapes are largely different from that of (R)-BINOL (**Fig. 15**) also supports that their CD spectra arise mainly from a conformation. **Fig. 28 B** shows the CD/UV spectra of poly(BINOL-*alt*-13DIB)s obtained at 50 and 100% e.e. of BINOL in feed. The CD spectral patterns are remarkably different from those of the linear dimers suggesting that the polymers' CD patterns reflect their helical conformation. Further, the two polymer CD spectra do not only different in intensity but also in spectral pattern from each other. The polymer obtained at 100% e.e. of BINOL in feed has all negative responses in the range of 225-267 nm while the one

obtained at 50% e.e. of BINOL in feed has a clear positive peak at 246 nm. These spectral features mean reflect that (R)- and (S)-BINOL units are in a diastereomeric relation in a helical chain as the same preferred-handed helicity in the two systems would be plausible. The differences in NMR spectra between the two systems (**Fig. 25 b** and **c**) may also arise from diastereomeric (R)- and (S)-BINOL units in a helical chain.

A. BINOL-1,3-DIB linear dimer

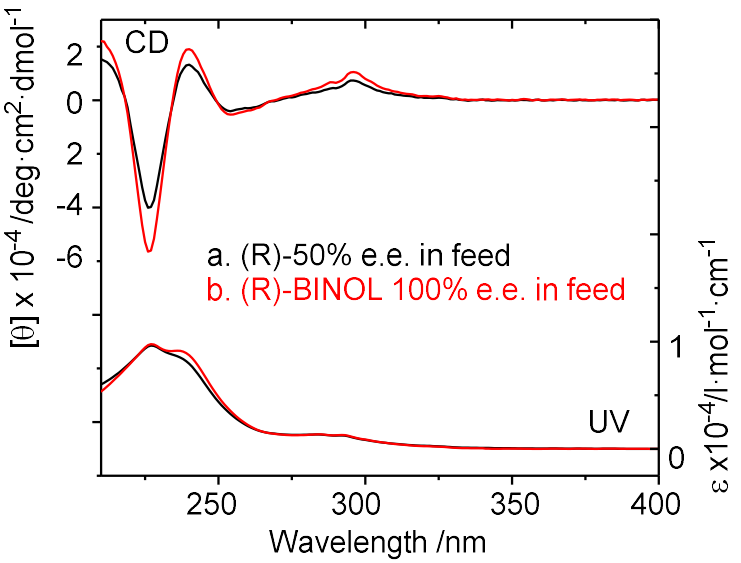

B. Poly(BINOL-*alt*-1,3-DIB)

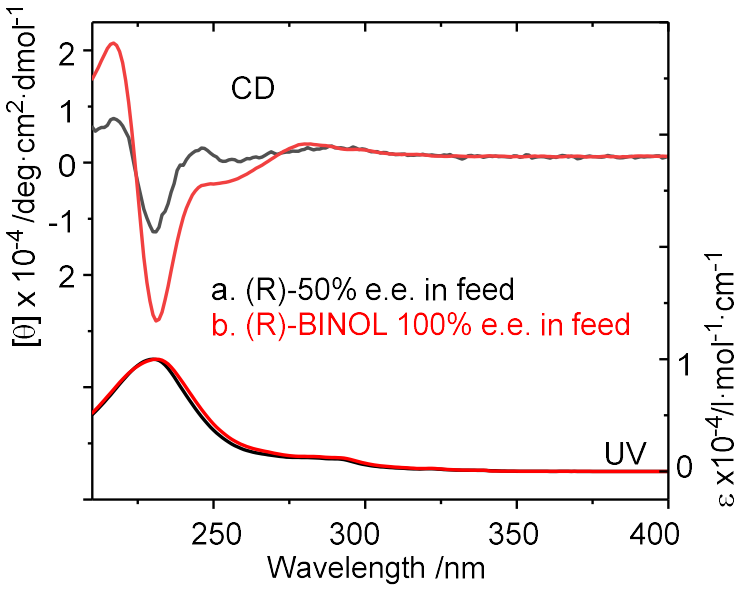

Fig. 28. CD spectra measured in THF solution of BINOL-13DIB linear dimers (A) and poly(BINOL-*alt*-13DIB) (B) obtained at 50% e.e. (M_n 3430) (a) and 100% e.e. (M_n 2840) (b) of (R)-BINOL in feed.

Another important feature of the CD spectra of poly(BINOL-*alt*-13DIB)s is found in intensity. The negative splitting centered at 217 nm is considered to be based mainly on the axial chirality of BINOL units, and the negative trough at 231 nm of the polymer obtained at 100% e.e. of BINOL in feed has a molar ellipticity of -2.6 deg $cm^{-2}dmol^{-1}$ which is about 3 times less in absolute value than that of the same band of poly(BINOL-*alt*-14DIB) obtained at 100% e.e. of BINOL (-7.2 deg $cm^{-2}dmol^{-1}$) and also than that of pure BINOL (-7.3 deg $cm^{-2}dmol^{-1}$) (**Fig. 15**). These results imply that the CD band of poly(BINOL-*alt*-13DIB) is contributed by helicity formed through the polymerization as well as BINOL unit chirality. The formation of helical conformation seems to create positive Cotton effects at around 231 nm.

Although the details of helical conformation of poly(BINOL-*alt*-13DIB) are not yet clear, possible conformations obtained by MD and MM calculations for the chain comprised only of (R)-BINOL units are shown in **Fig. 29**. The proposed structures are characterized left-handed helical sharp turns based on chirality of (R)-BINOL (2/1-helical motif) which are arranged also in a left-handed, single-handed helical manner with greater pitches (9/1 in A and 8/1 in B). Although the calculated steric energy of conformation A was lower (2202 kcal mol^{-1}) than that of B (2328 kcal mol^{-1}), the difference seems not large enough to identify A as the most probable structure. However, the sharp turn structures based on BINOL were almost unchanged in the two models through the MD simulations; the actual helical conformation would be characterized by the sharp left-handed, local turns forming a longer-pitched, left-handed helical chain.

A.Poly(BINOL-*alt*-13DIB) [9/1-helix]

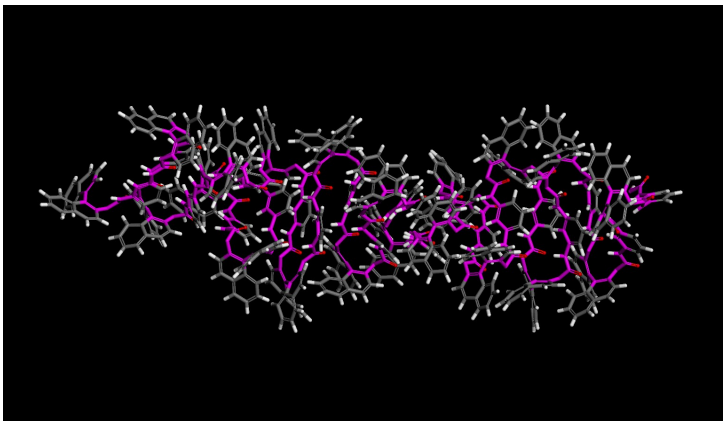

B. Poly(BINOL-*alt*-13DIB) [8/1-helix]

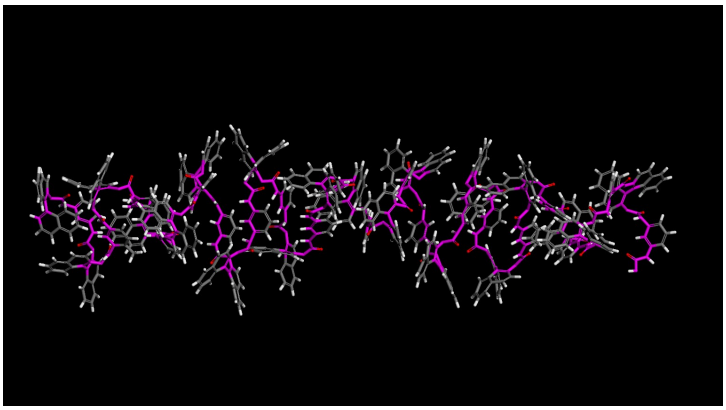

Fig. 29. Possible conformations of poly(BINOL-*alt*-13DIB) consisting of R-BINOL units obtained by MD simulations for 14-16 nsec at 297K followed by MM optimization using COMPASS force field.

The two conformations of poly((R)-BINOL-*alt*-13DIB) are remarkably different from the left-handed 2/1-helical structure of poly((R)-BINOL-*alt*-14DIB) in the fact that average distance between benzene-1,3-diyl moieties appeared too long to form π-stacked structure (5.66 Å for 9/1-helix and 6.37 Å for 8/1-helix in **Fig. 29**) (**Fig. 30**). The corresponding distance for poly poly((R)-BINOL-*alt*-14DIB) was 4.53 Å.[11] These structural features are in line with the ^{1}H NMR spectral patterns of the two polymers indicating that

poly((R)-BINOL-*alt*-14DIB) has π-stacking while poly((R)-BINOL-*alt*-13DIB) does not at least in solution.

A. 9/1-Helix

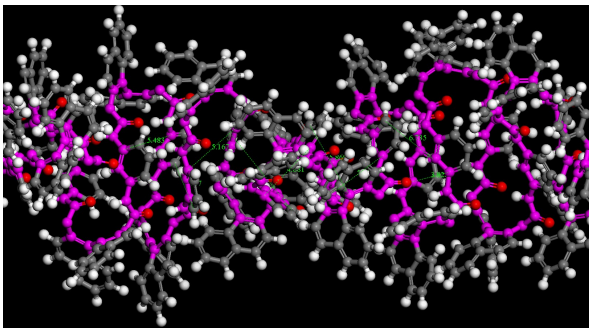

B. 8/1-Helix

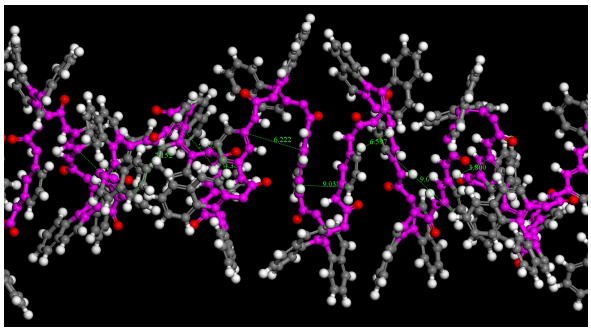

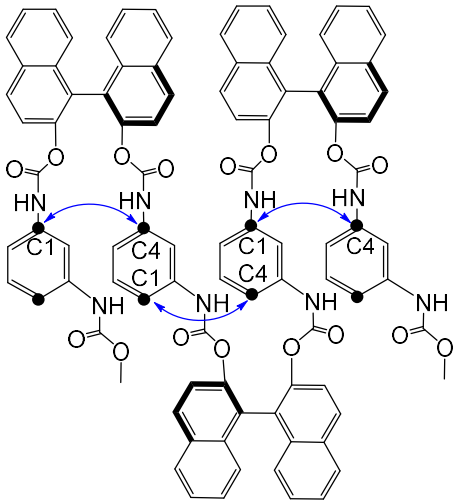

Fig. 30. Optimized conformations of poly((R)-BINOL-*alt*-13DIB) 20-mer, 9/1-helix (A) and 8/1-helix (B) with measured distances between between C1 and C4 of neighboring benzene-1,3-diyl units. The central nine units starting from the sixth one form a terminal were selected for distance measurements to avoid terminal effects. The averaged distances were 5.66 Å in A and 6.37 Å in B.

On the other hand, WAXD profile of poly(BINOL-*alt*-13DIB) showed a peak at 2θ of 21.5 deg corresponding to a d-spacing of 4.13 Å (**Fig. 31**). This result may mean that poly((R)-BINOL-*alt*-13DIB) has a π-stacking character in the solid state while stacking was not supported by NMR in solution. The conformation of poly(BINOL-*alt*-13DIB) may be more flexible than that of poly(BINOL-*alt*-14DIB) in solution and may be stabilized in the solid state. It is noteworthy that the WAXD pattern of poly(BINOL-*alt*-13DIB) was broader than that of poly(BINOL-*alt*-14DIB), suggesting that the conformation of poly(BINOL-*alt*-13DIB) is less ordered that that of poly(BINOL-*alt*-14DIB) in the solid state. In addition, poly(BINOL-*alt*-13DIB) did not show any clear melting point in DSC analysis, suggesting that there is no regular chain packing of the polymer in the solid state (**Figs. 32** and **33**). This aspect reinforces that the aforementioned WAXD peak is ascribed to intramolecular π-stacking.

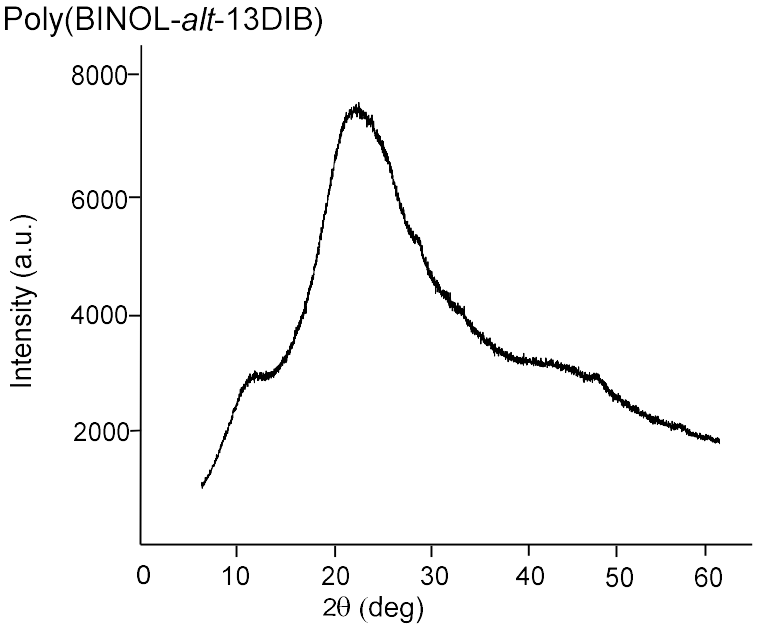

Fig. 31. WAXD profiles of poly(BINOL-*alt*-13DIB) (M_n 2460). [RIGAKU Miniflex diffractometer, CuKα, 30 KV, 10 mA, scan speed 1.25 degree/min, step 0.01 degree]

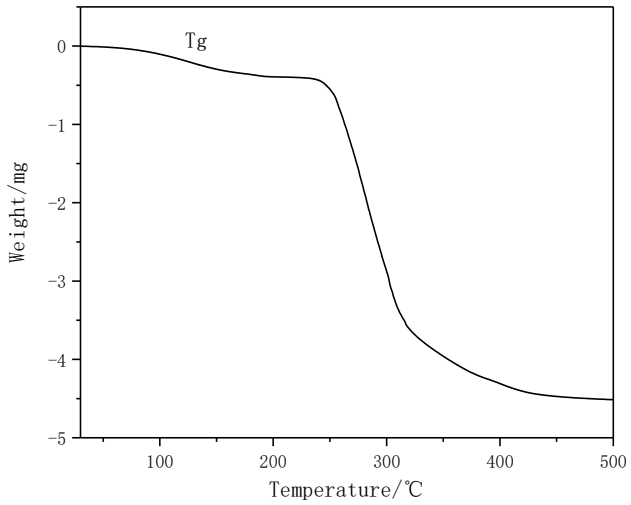

Fig. 32. DT-TGA profiles of poly(BINOL-*alt*-13DIB) (M_n 2460) (B) obtained at 100% e.e. of (*R*)-BINOL in feed [heating scan rate: 10 deg/min].

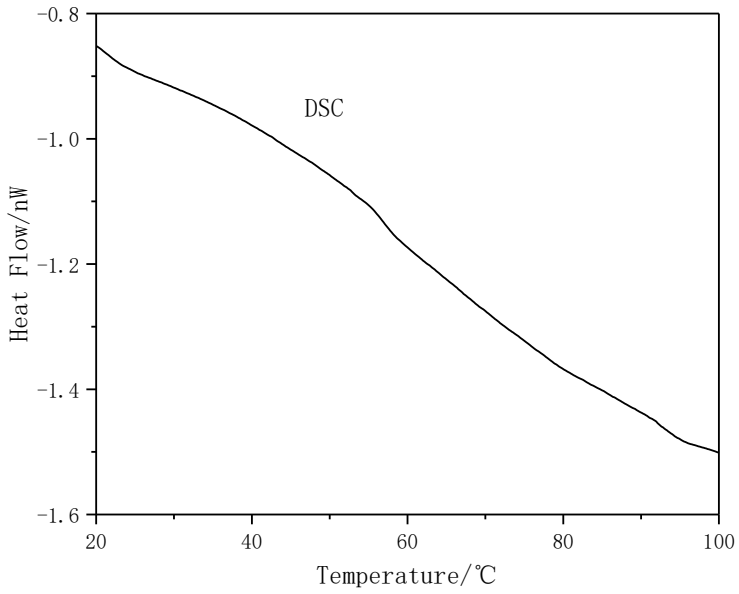

Fig. 33. DSC profiles of poly(BINOL-*alt*-13DIB) (M_n 2460) (B) obtained at 100% e.e. of (*R*)-BINOL in feed [2nd heating scan at 10 deg/min].

Conclusions

In a sharp contrast to the BINOL-14DIB systems, the BINOL-13DIB systems did not produce cyclic dimers but linear dimers as major components of dimer. The content of linear dimers was almost constant regardless of e.e. of BINOL in feed. In addition, poly(BINOL-*alt*-13DIB) is proposed to compose of sequences with rather more randomly distributed (R)- and (S)-BINOL units than those in poly(BINOL-*alt*-14DIB). CD spectra of poly(BINOL-*alt*-13DIB)s seem to be contributed by bands reflecting helical chirality which overlaps the negative splitting due to (R)-BINOL chirality. Further, a chain conformation is proposed to be characterized by sharp, left-handed turns based on BINOL chirality forming a longer-pitched, left-handed helix with no intra-chain π-stacking character for poly((R)-BINOL-*alt*-13DIB) in solution which is in sharp contrast to the left-handed 2/1-helical conformation of poly((R)-BINOL-*alt*-14DIB) with intra-chain π-stacking. Both poly((R)-BINOL-*alt*-13DIB) and poly((R)-BINOL-*alt*-14DIB) has π-stacking in the solid state as indicated by WAXD analysis.

Thus, the different substitution positions in the benzene ring which is the only and subtle difference between the BINOL-14DIB and BINOL-13DIB systems results in remarkable differences in polymerization behaviors and sequence structures and chiroptical properties of the reaction products. While reports on polyurethanes from a view of stereostructure are very rare, this work presents the systematic, in-depth studies of helical polyurethanes. Once fine stereochemical control is performed over polyurethanes, they may find a wide range of applications in advanced chiral materials on the basis of the advantages that polyurethanes can be prepared by simple polyaddition under mild conditions, that chemical structural variations can be readily introduced by changing diol and diisocyanate monomers, and that polyurethanes can interact through hydrogen bonds

using the urethane group with external polymers and molecules.

Experimental

Materials. 1,3-diisocyanatobenzene (TCI), (*R*)-(+)-1,1'-bi-2-naphthol (TCI) were used as purchased. Tetrahydrofuran (Kanto Chemical) was dried with sodium benzophenone ketyl and distilled immediately before use under N_2. Et_3N was distilled over CaH_2 and stored over KOH under nitrogen.

Synthesis of Poly(BINOL-*alt*-13DIB). The synthetic procedure is described for the system with (R)-BINOL at 50% e.e. is described. To a solution of (*R*)-(+)-1,1'-bi-2-naphthol (0.1 g, 0.35 mmol) in THF (2 mL) were added 1,3-diisocyanatobenzene (0.056 mg, 0.35 mmol) and triethylamine (0.11 mL, 0.79 mmol) in this order under nitrogen atmosphere. The mixture was stirred for 24 h at room temperature and terminated by exposure to air. The polymer and cyclic dimer were isolated and purified by preparative SEC. SEC (vs. standard polystyrenes): M_n 3430, M_w/M_n 1.24. FT-IR (KBr) υ/cm^{-1}: 3391, 3062, 2922, 1733, 1610, 1535, 1508, 1492, 1471, 1457, 1427, 1359, 1307, 1192, 1076, 1038, 1016, 970, 772, 749.

General instrumentation. ^1H NMR spectra were recorded on a JEOL JNM-ECX400 spectrometer (400 MHz for ^1H measurement) and a JEOL JNM-ECA600 spectrometer (600 MHz for ^1H measurement). SEC measurements were carried out using a chromatographic system consisting of a Hitachi L-7100 chromatographic pump, a Hitachi L-7420 UV detector (254 nm), and a Hitachi L-7490 RI detector equipped with TOSOH TSK gel G6000H_{HR} and G3000H_{HR} columns (30 x 0.72(i.d.) cm) connected in series (eluent THF, flow rate 1.0 mL/min). SEC analyses were also carried out at room temperature using a chromatographic system consisting of a JASCO PU-2080 PLUS intelligent HPLC pump, a JASCO UV-2075 PLUS intelligent UV/Vis detector (254 nm), a JASCO RI-930 intelligent RI detector, and a JASCO CO-1565 intelligent column oven (23 ºC) equipped with TOSOH TSK gel G6000H_{HR} and G3000H_{HR} columns (30 x 0.72(i.d.) cm) connected in series (eluent $CHCl_3$, flow rate 1.0 mL/min). Preparative SEC separation of dimers was performed using a JAI LC-908 preparative recycle chromatograph equipped with JAIGEL-1H and JAIGEL-2H columns connected in series (eluent $CHCl_3$). Chiral HPLC was performed using chromatographic system consisting of a JASCO DG-980-50 degasser, a JASCO PU-980 pump, a JASCO CD-2095plus CD detector, and a JASCO UV-2070plus UV detector equipped with a Daicel Chiral Pak IA column (25 cm x 0.46 cm (i.d.)) [eluent CH_2Cl_2-hexane (95/1), flow rate 0.5 mL/min]. UV-vis absorption spectra were measured at room temperature with a JASCO V-550 and V-570 spectrophotometers. Steady-state emission spectra were taken on a JASCO FP-8500 fluorescence spectrophotometer. IR spectra were recorded on a JASCO FT/IR-6100

spectrometer using KBr pellet samples. Circular dichroism (CD) and linear dichroism (LD) spectra were taken with a JASCO-820 spectrometer. The spectra were obtained by averaging those recorded at four (90^{o} interval) or two (180^{o} interval) different film orientations (angles) with the film face positioned vertically to the incident light beam for measurement. Linear dichroism contributions were thus minimized to afford true CD spectra. Differential scanning calorimetry (DSC) and thermal gravity analysis (TGA) were taken on Rigaku Thermo Plus DSC8230 and TG8120 analyzer at a heating rate of 10 K/min in nitrogen atmosphere. WAXD measurement was performed on a RIGAKU Miniflex diffractometer.

Computational method. Wave-form analysis of SEC curves for determination of the contents of polymers and dimers were performed using Origin 2018 software package (Origin Lab). Molecular mechanics structure optimization was conducted using the COMPASS force field implemented in the Discover module of the Material Studio 4.2 (Accelrys) software package with the Fletcher-Reeves conjugate gradient algorithm until the RMS residue went below 0.01 kcal/mol/Å. Molecular dynamic simulation was performed under a constant NVT condition in which the numbers of atoms, volume, and thermodynamic temperature were held constant. Berendsen's thermocouple was used for coupling to a thermal bath. The step time was 1 fs and the decay constant was 0.1 ps. Conformations obtained through MD simulation were saved in trajectory files at every 5 or 10 ps and were optimized by MM simulation.

References

(1) E. Yashima, N. Ousaka, D. Taura, K. Shimomura, T. Ikai and K. Maeda, *Chem. Rev.*, 2016, **116**, 13752-13990.

(2) E. Yashima, K. Maeda, H. Iida, Y. Furusho and K. Nagai, *Chem. Rev.*, 2009, **109**, 6102-6211.

(3) T. Nakano and Y. Okamoto, *Chem. Rev.*, 2001, **101**, 4013-4038.

(4) T. Nakano, *J. Chromatogr. A*, 2001, **906**, 205-225.

(5) Y. Okamoto and T. Nakano, *Chem. Rev.*, 1994, **94**, 349-372.

(6) J. Shen and Y. Okamoto, *Chem. Rev.*, 2015, **116**, 1094-1138.

(7) T. Nakano, *Chem. Rec.*, 2014, **14**, 369-385.

(8) R. Wang, Y. Zheng, X. Li, J. Chen, J. Cui, J. Zhang and X. Wan, *Polym. Chem.*, 2016, **7**, 3134-3144.

(9) Z. Yu, X. Wan, H. Zhang, X. Chen and Q. Zhou, *Chem. Commun.*, 2003, 974-975.

(10) J. Cui, J. Zhang and X. Wan, *Chem. Commun.*, 2012, **48**, 4341-4343.

Chapter 4. Synthesis, Structure and Properties of Polyurethane Prepared from 2,7-Diisocyanatofluorene and Optically Pure 1,1'-Bi-2-naphthol: Directional Control over Helical Chain

Introduction

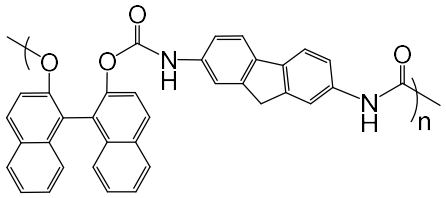

Poly(BINOL-*alt*-27DIF)

Chirality of macromolecules plays important roles in a wide variety of polymeric materials.[1-10] Optically active macromolecules may have chiral configuration and chiral conformation (helix) prepared through asymmetric chirogenic polymerization and asymmetric helix-chirogenic polymerization (helix-sense-selective polymerization), respectively, where chain asymmetry can be induced to the chain typically using chiral ligands or chiral monomers. As an example of asymmetric helix-chirogenic polymerization (helix-sense-selective polymerization), we have recently reported the synthesis of 2/1-helical polyurethanes with single-handed helicity from 1,3- or 1,4-diisocyanatobenzene (13DIB or 14DIB) and (*R*)- or (*S*)-2,2'-dihydroxy-1,1'-binaphthyl (BINOL) (poly(BINOL-alt-13DIB) or poly(BINOL-alt-14DIB). The 2/1-helical conformation is based on the axial chirality of BINOL which introduces and stabilizes turn structures to the chain, and (*R*)-absolute configuration of BINOL units yields left-handed helicity. In addition to the helical feature, the polymer chain is characterized by π-stacked arrangement of -C(O)NH-C_6H_4-NHC(O)- moieties.

This chapter introduces a new helical polyurethane derived from optically active BINOL at and 2,7-diisocynanatofluorene (27DIF) (poly(BINOL-*alt*-27DIF)) (Scheme 1). Unlike the aforementioned poly(BINOL-*alt*-14DIB), poly(BINOL-*alt*-27DIF) can have an

additional stereochemical feature due to relative orientation of the carbamate moieties [-C(O)NH-fluorene-2,7-diyl-NHC(O)-]. The fluorene-2,7-diyl moieties form π-stacking in which two different arrangements of fluorene units are possible, i.e., the 9-position methylene groups of two fluorene-2,7-diyl moieties may point to the same side of the chain (syn-arrangement) leading to "parallel helix" or they may point to the opposite sides of the chain (anti-arrangement) leading to "anti-parallel helix". Stereostructure of the poly(BINOL-*alt*-27DIF) was investigated with a focus on this aspect. Though various helical polymers have been synthesized, parallel and anti-parallel chains based on relative, local conformational arrangements of chain components have never been observed or controlled for synthetic polymers to the best of our knowledge while parallel and anti-parallel chains based on the opposite directions of monomeric units have been well established for β-sheet peptides. Control over such structural features which have never been noticed in synthetic polymer research may open a way to unforeseen structure-property scopes of polymeric materials. In addition, due to the presence of fluorene units, the polymer may be potentially interesting as material emitting circular polarized light (CPL).

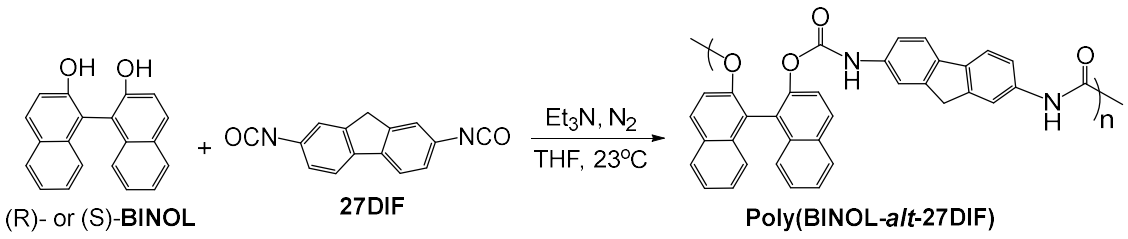

(R)- or (S)-**BINOL** **27DIF** **Poly(BINOL-*alt*-27DIF)**

Scheme 1. Syntheses of polyurethane from BINOL and 27DIF.

Results and discussion

The polymerization of 27DIF with (R)-BINOL or (S)-BINOL at 100% e.e. was conducted

in dried tetrahydrofuran (THF) containing 5 % of Et_3N as a reaction promoter in the presence of a small amount of added water. The product was purified by preparative size-exclusion chromatography (SEC). While a significant amount of cyclic dimers were formed and they were isolated in the synthesis of poly(BINOL-alt-14DIB), the amount of short oligomeric species possibly including cyclic dimer appeared to be much lower in the polymerization systems of 27DIF and BINOL.

It was found that a small amount of water affects the stereochemistry of polymerization; however, a small amount of water did not hamper polymerization reaction, and molar mass dispersity of the product obtained in the presence of 0.17 eq water was similar to that of the product obtained in the absence of water (Fig. 1). Fig. 2 A and B shows the circular dichroism (CD)/UV spectra of poly((*R*)-BINOL-*alt*-27DIF). The polymer in Fig. 2 A was obtained in dry THF while the one in Fig. 2 B in THF containing 0.17 eq. of water with respect to 27DIF at [27DIF] = [BINOL] = 0.154 M at 23ºC. The reactions in the absence and the presence of water led to almost complete consumption of the monomers and resulted in similar molar mass distribution of the products, indicating that a small amount of water did not hamper propagation of polymer chains.

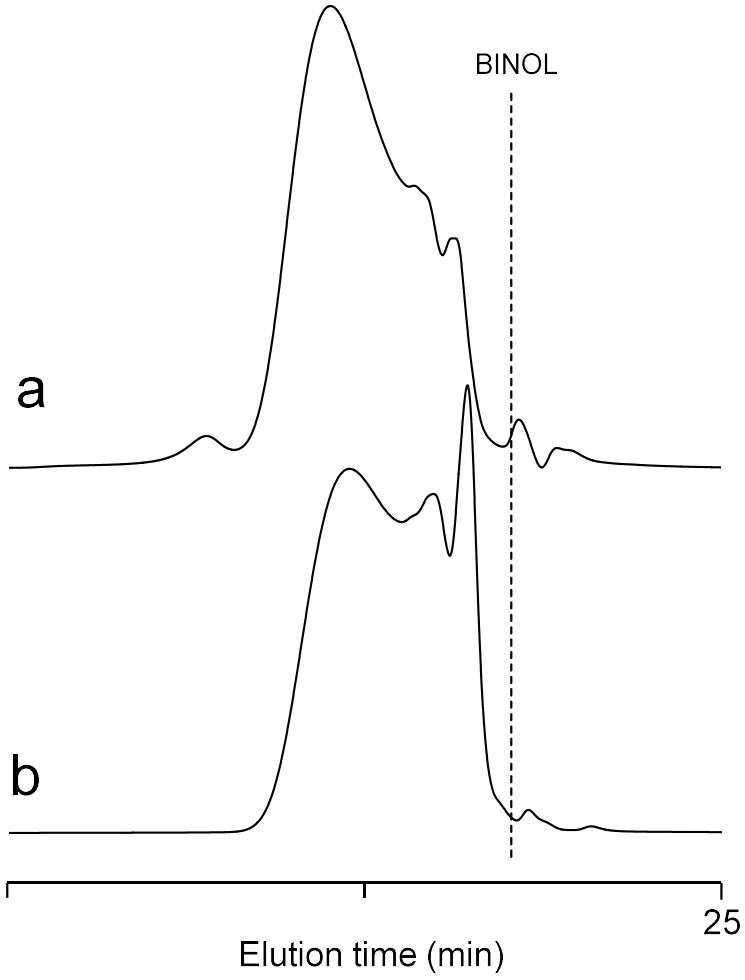

Fig. 1. SEC profiles of polymerization products at [27DIF] = [BINOL] = 0.154 M at 23°C in dry THF (a) and in THF containing 0.17 eq. water.

The polymers exhibited intense CD spectra whose patterns were significantly different form that of (*R*)-BINOL, suggesting that the polymers have conformational chirality (helix) induced through the polymerization on the basis of chirality of BINOL. It is also noteworthy that the spectra of the polymer obtained in the anhydrous condition and that obtained in the presence of a small amount of water are not alike at all. This aspect strongly suggests that there are two different helical conformations possible of poly(BINOL-*alt*-27DIF) synthesized from the BINOL of the same handedness.

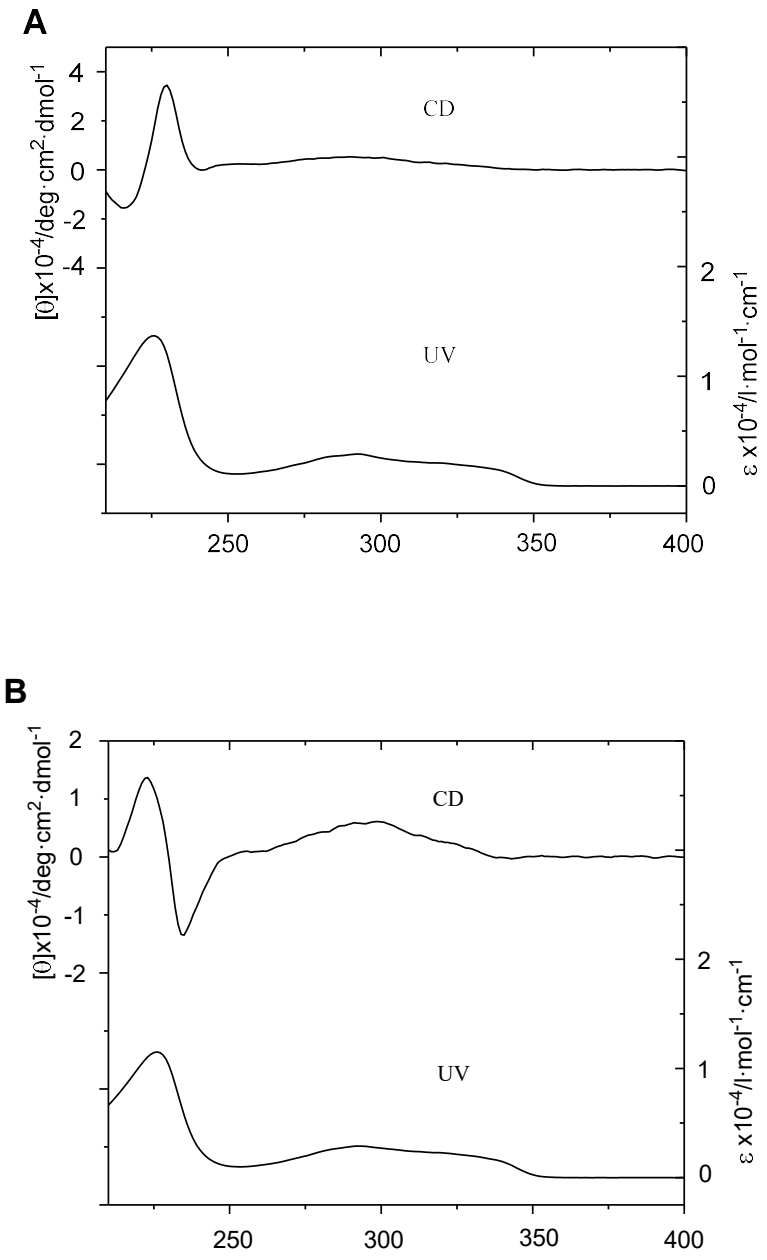

Fig. 2. CD-UV spectra of poly((R)-BINOL-*alt*-27DIB) synthesized at [27DIF] = [BINOL] = 0.154 M at 23ºC and purified by preparative SEC; the sample prepared in dry THF (M_n 3340) (a) and the sample prepared in THF containing 0.17 eq. water (M_n 2580) (b).

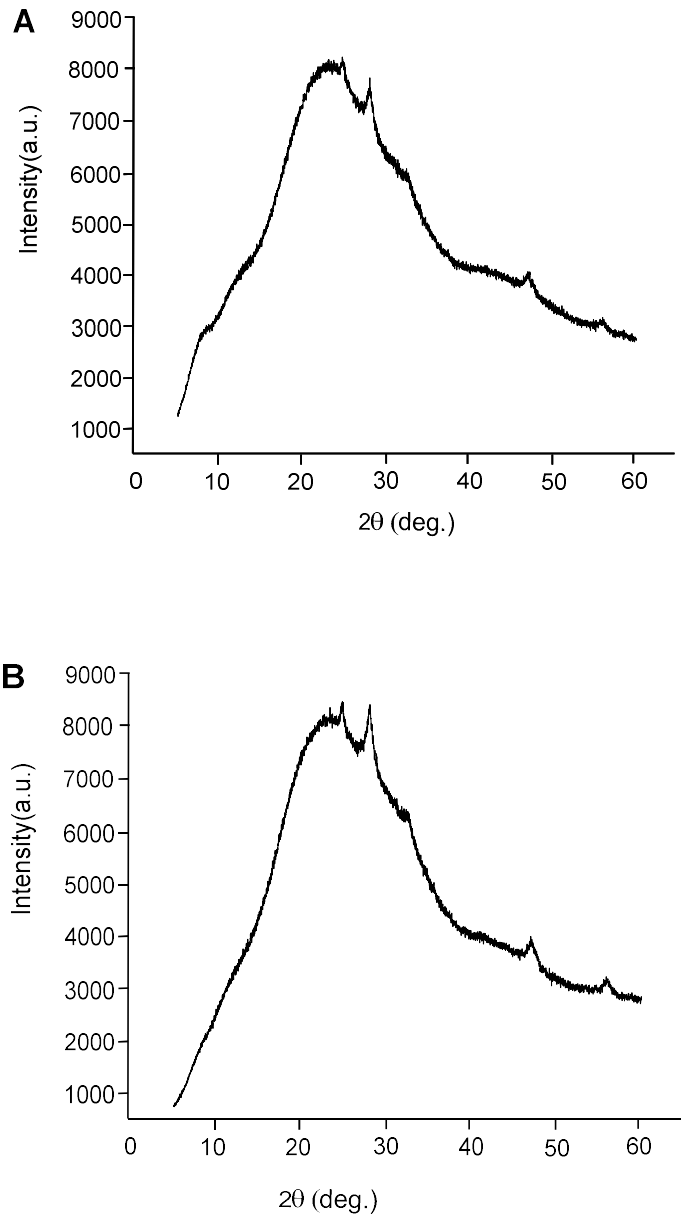

Fig. 3. XRD profiles of poly((R)-BINOL-*alt*-27DIB) synthesized at [27DIF] = [BINOL] = 0.154 M at 23ºC and purified by preparative SEC; the sample prepared in dry THF (M_n 3340) (a) and the sample prepared in THF containing 0.17 eq. water (M_n 2580) (b).

In addition, the two polymers in the solid state exhibited clear XRD profiles which showed a reflection signal at a d-spacing of ca. 4.44 Å (Fig. 3 A, B). Since no melting point was observed in the differential scanning calorimetry (DSC) analysis of the polymers, the d-spacing value would be ascribed to intramolecular (intrachain) π-stacked arrangement of fluorene-2,7-diyl groups in a helical chain. A similar XRD pattern has been reported for 2/1-helical poly(BINOL-alt-14DIB).

Based on these entries of information, two chain models of 20-mer were proposed and simulated by molecular dynamics for 10 nsec at 298ºC (Fig. 4 A, B). The two structures are 2/1-helical conformations where (R)-BINOL units lead to left-handed helicity with different relative arrangements of the π-stacked fluorene-2,7-diyl moieties. One has the 9-position methylene groups of two fluorene-2,7-diyl moieties pointing to the opposite sides of the chain (anti-arrangement) leading to “anti-parallel helix” (Fig. 4 A), and the other has the methylene groups pointing to the same side of the chain (syn-arrangement) leading to “parallel helix” (Fig. 4 B). The simulated anti-parallel helix had a more stretched conformation where the extent of overlapping of fluorene moieties appears less compared with the simulated parallel helix. The conformations were well maintained through the simulations, implying that they are stable enough.

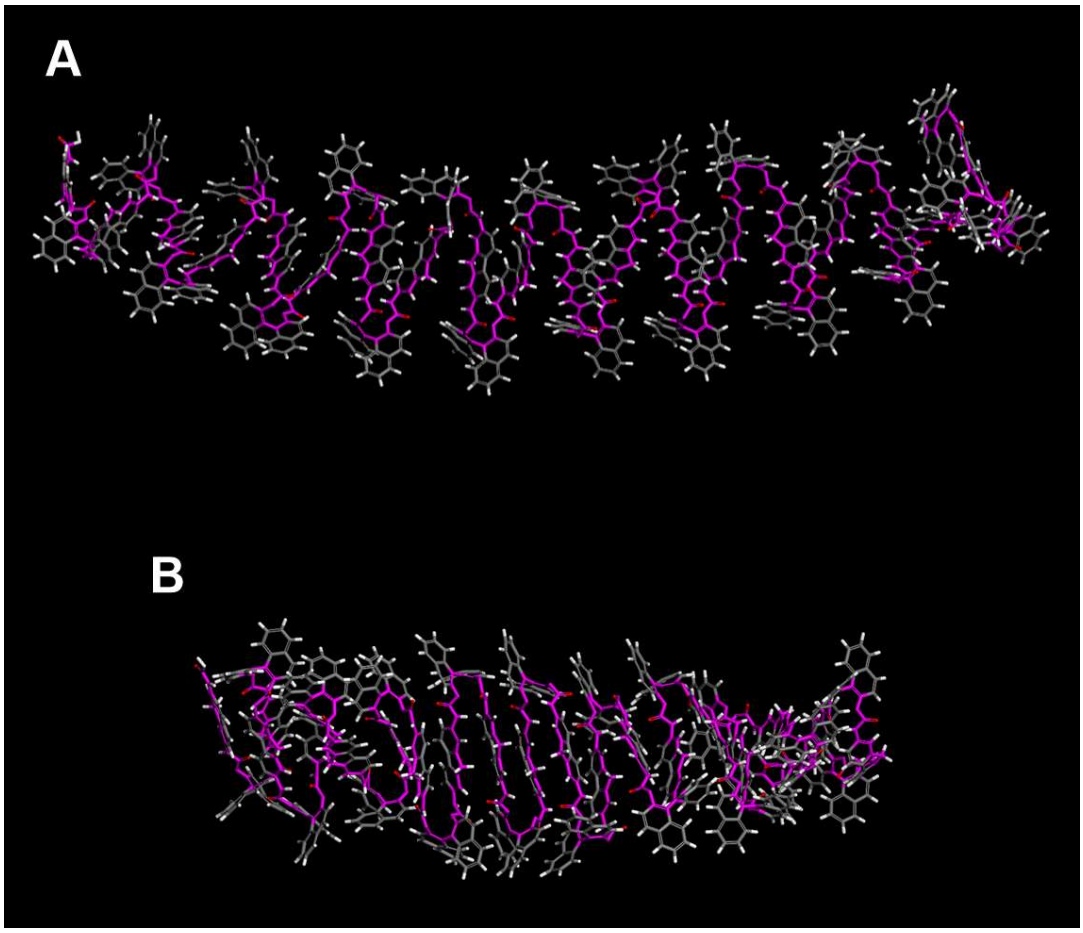

Fig. 4. Conformations of anti-parallel helix (A) and parallel helix (B) of poly((*R*)-BINOL-alt-27DIF) obtained through MD simulations at 298 K for 10 nsec.

In order to understand the correlation between the two different patterns of CD spectra shown in Fig.1 A and B and the two conformations, DFT calculations of CD spectra were performed for dimeric species models having two different arrangements of the fluorene-2,7-diyl moieties, i.e., syn- and anti-conformations (Fig. 5 A and B). The theoretical CD spectrum for the anti-conformation (Fig. 5A) and that of the syn-conformation (Fig. 5 B) were rather similar to the experimental spectra in Fig. 2 A and B, respectively. These results strongly suggest that the polymerization in dry THF yields mainly the anti-

arrangement of fluorene-2,7-diyl moieties leading to anti-parallel helix while the presence of a small amount of water changes the reaction stereochemistry to yield mainly the syn-arrangement of fluorene-2,7-diyl moieties leading to parallel helix.

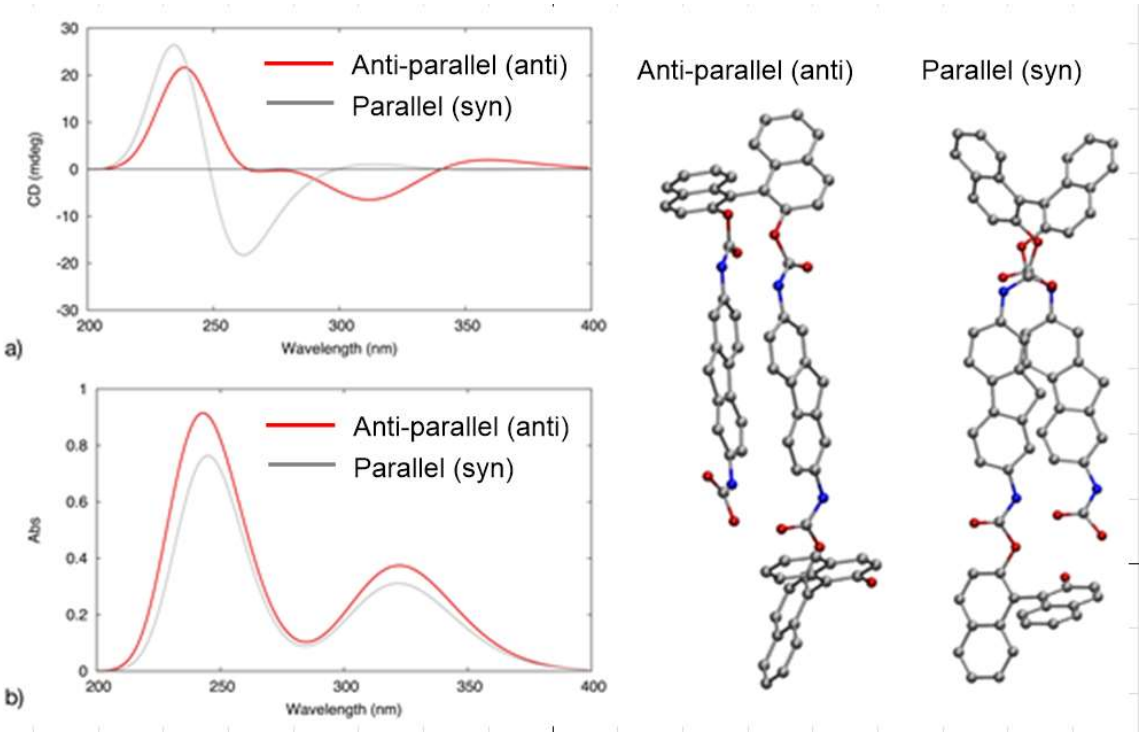

Fig. 5. Theoretical CD (top) and UV (bottom) spectra of dimeric models of anti-parallel (anti) and parallel (syn) helical chains.

Stability of the two conformations were tested on heating polymer solutions in THF at 60°C for 30 h. No clear changes were observed in CD or UV spectra of the polymers, indicating that the two conformations are stable and that interchange between the two does not occur under the examined conditions. In search for reaction conditions that may affect the polymerization stereochemistry, it was found that polymerization in dry THF led to anti-parallel helix regardless of reaction temperature (-20°C, 23°C) and monomer

concentration ([27DIF] = [BINOL] = 0.070 M, 0.154 M, 0.300 M) where CD intensity was almost constant. Also, reactions in the presence of 1.5 eq. and 2.4 eq. water led to parallel helix as well as that with 0.17 eq. water where over all molar-mass of the products significantly decreased with an increase in the amount of H_2O while CD intensity was not seriously affected by the amount of H_2O.

The role of water should be clarified. In order obtain information on this point, NMR studies to find out any interactions between water and 27DIF or between water and BINOL (Fig. 6). While no shifts of signals were confirmed for 27DIF on the addition of water, the signal based on -OH group of BINOL showed a clear up-field shift in the presence of water probably due to H-bonding interactions. These results may mean that the growing reaction species involving BINOL terminal group bound by water through H-bonding and free BINOL lead to parallel and anti-parallel helices, respectively. Further studies including theoretical analyses will be necessary to shed light on more detailed mechanism of stereo control.

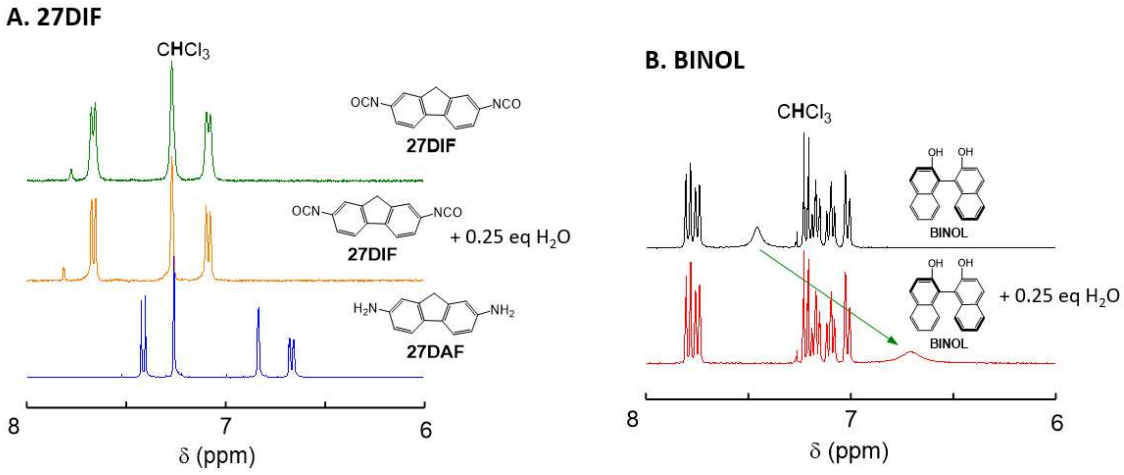

Fig. 6. ^{1}H NMR spectra of 27DIF (**A**) and (*R*)-BINOL (**B**) in THF-Et_3N-$CDCl_3$ (0.4 mL/0.02mL/0.1 mL) in the absence of H_2O and in the presence of 0.25 eq. H_2O [400 MHz, r.t.]

The anti-parallel and parallel structures showed very similar IR spectra (Fig. 7). This observation confirms that the two polymers have the same chemical structure and they differ only in conformation.

On the other hand, the anti-parallel and parallel structures led to distinguishable ^{1}H and ^{13}C NMR spectra (Fig. 8). Both spectra led to different spectral patterns of, which may arise from different stereo structures of the polymer chain.

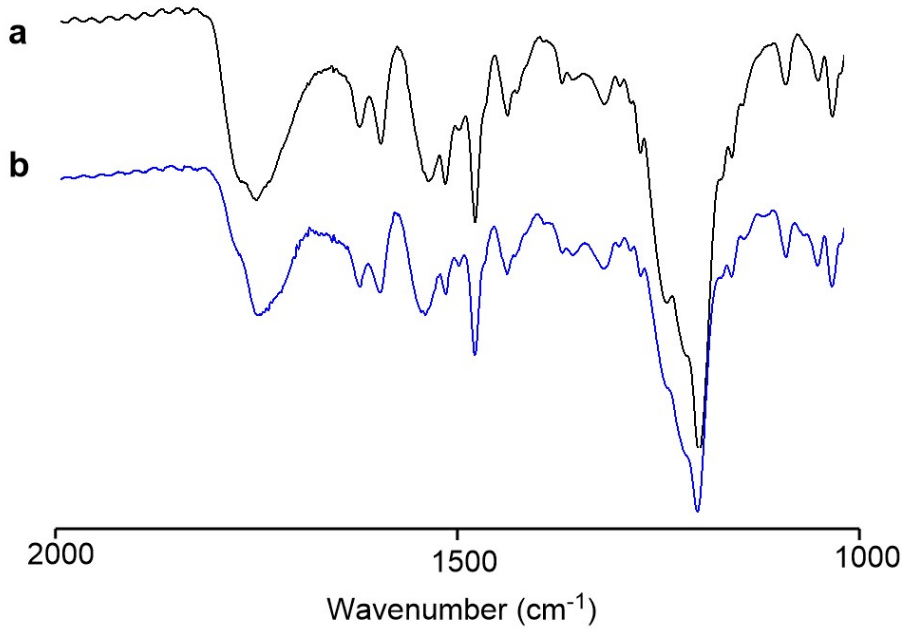

Fig. 7. IR spectraof poly((R)-BINOL-*alt*-27DIB)s synthesized at [27DIF] = [BINOL] = 0.154 M at 23ºC and purified by preparative SEC; the sample prepared in dry THF (M_n 3340) (a) and the sample prepared in THF containing 0.17 eq. water (M_n 2580) (b). [400 MHz (H) and 125 MHz (C), $CDCl_3$, 23ºC]

In addition, fluorescence spectral shape and intensity were significantly affected by anti-parallel/parallel directions of helical chain (Fig. 9). The solution spectra comprise of a shaper band centered at around 360 nm and a broader band centered at around 430 nm which may be ascribed to monomer and excimer emissions, respectively, of fluorene moieties. The anti-parallel helix in solution (Fig. 9 A) had a higher intensity ratio of the monomer emission band compared with the parallel helix in solution (Fig. 9 B). This observation is consistent with the MD simulation results that the simulated anti-parallel chain had a less extent of π-stacking than the simulated parallel chain.

CPL measurements were performed for the polymer solutions: however, only very weak CPL was confirmed for the anti-parallel helical polymer and almost no CPL was observed for the parallel helical polymer.

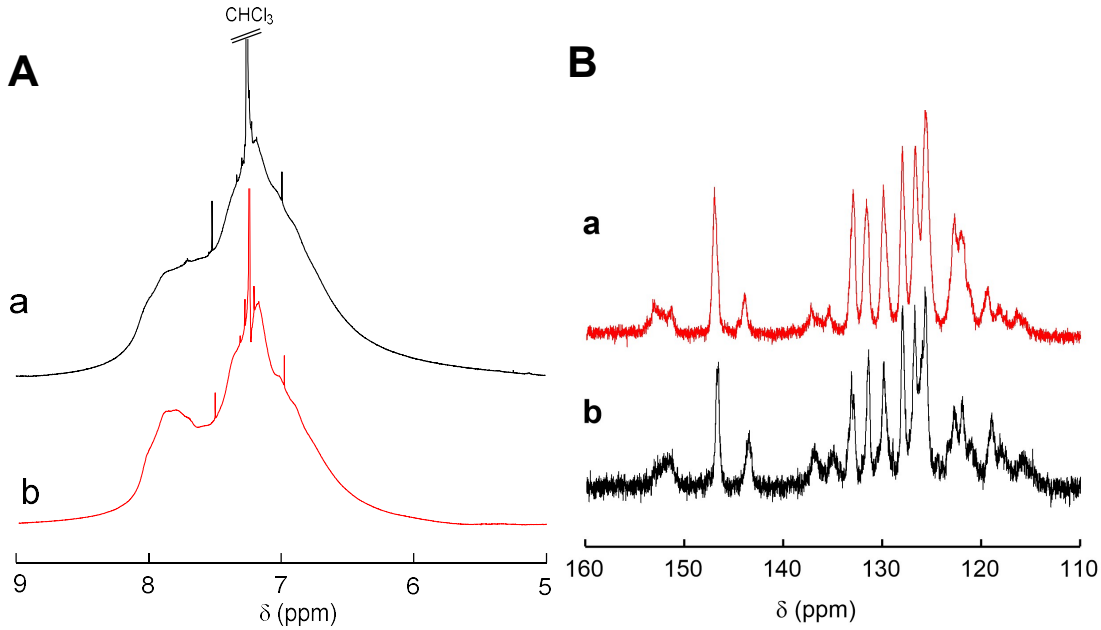

Fig. 8. [1]H NMR spectra (A) and 13C NMR spectra (B) of poly((R)-BINOL-*alt*-27DIB)s synthesized at [27DIF] = [BINOL] = 0.154 M at 23°C and purified by preparative SEC; the sample prepared in dry THF (M_n 3340) (a) and the sample prepared in THF containing 0.17 eq. water (M_n 2580) (b). [400 MHz (H) and 125 MHz (C), $CDCl_3$, 23°C]

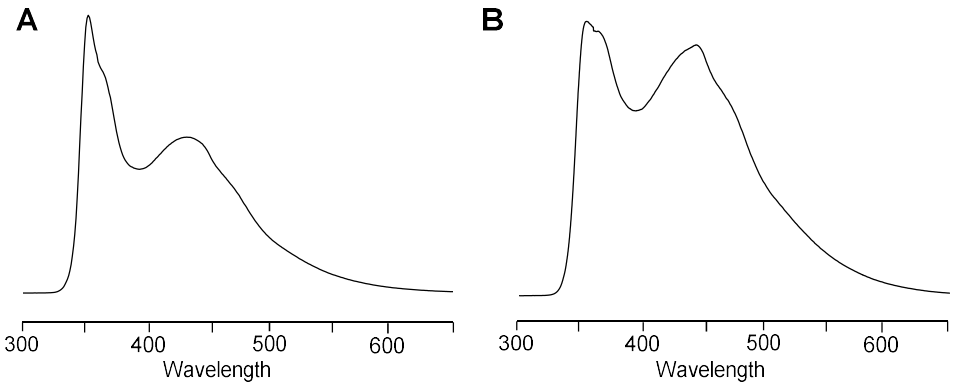

Fig. 9. Fluorescence spectra of poly((R)-BINOL-*alt*-27DIB) in THF solution: anti-parallel helix (M_n 3340) (A) parallel helix (M_n 2580) (B). [conc. 1.0 x 10^{-6} M in THF, 1-cm cell, λ_{ex} 277 nm].

Conclusions

Polyaddition between BINOL and 27DIF afforded an optically active polyurethane having fluorescent fluorene-2,7-diyl moieties incorporated in the main chain. The polymer was proposed to have 2/1-helical conformations with variations of relative arrangements of fluorene-2,7-diyl moieties, i.e., "parallel helix" with the 9-position methylene groups of two fluorene-2,7-diyl moieties point to the same side of the chain (syn-arrangement) leading and "anti-parallel helix" with the methylene groups point to the opposite sides of the chain (Fig. 9). The two directions of helical chain is controlled by reaction conditions; reaction in dry THF leads to anti-parallel helix while reaction in THF containing a small amount of water to parallel helix.

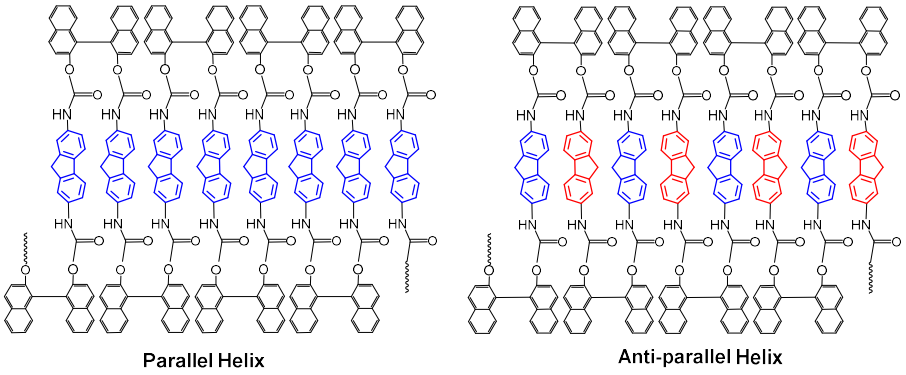

Fig. 9. Schematic representations of parallel helix and anti-parallel helix.

The assignment of two types of helices was conducted through theoretical calculations of CD and UV spectra in collaboration with Professor Adriana Pietropaolo (University of Catanzaro, Italy). The two helices led to distinguishable fluorescent spectral profiles. While there have been a variety of examples of synthetic, helical polymers, identification and control of parallel and anti-parallel helices are considered unprecedented.

Experimental

Materials. 2,7-Diaminofluorene (TCI), (*R*)-(+)-1,1'-bi-2-naphthol (TCI) were used as purchased. Tetrahydrofuran (Kanto Chemical) was dried with sodium benzophenone ketyl and distilled immediately before use under N_2. Et_3N was distilled over CaH_2 and stored over KOH under nitrogen.

Synthesis of Poly((*R*)-BINOL-*alt*-27DIF). The synthetic procedure is described for the system with (R)-BINOL at 100% e.e. is described. To a solution of (*R*)-(+)-1,1'-bi-2-naphthol (0.1 g, 0.35 mmol) in THF (2 mL) were added 2,7-diisocyanatofluorene (0.056 mg, 0.35 mmol) and triethylamine (0.11 mL, 0.79 mmol) in this order under nitrogen atmosphere. The mixture was stirred for 24 h at room temperature and terminated by exposure to air. The polymer and cyclic dimer were isolated and purified by preparative SEC. SEC (vs. standard polystyrenes): M_n 2780, M_w/M_n 1.24. FT-IR (KBr) υ/cm^{-1}: 3391, 3062, 2922, 1733, 1610, 1535, 1508, 1492, 1471, 1457, 1427, 1359, 1307, 1192, 1076, 1038, 1016, 970, 772, 749.

General instrumentation. ^1H NMR spectra were recorded on a JEOL JNM-ECX400 spectrometer (400 MHz for ^1H measurement) and a JEOL JNM-ECA600 spectrometer (600 MHz for ^1H measurement). SEC measurements were carried out using a chromatographic system consisting of a Hitachi L-7100 chromatographic pump, a Hitachi L-7420 UV detector (254 nm), and a Hitachi L-7490 RI detector equipped with TOSOH TSK gel G6000H_{HR} and G3000H_{HR} columns (30 x 0.72(i.d.) cm) connected in series (eluent THF, flow rate 1.0 mL/min). SEC analyses were also carried out at room temperature using a chromatographic system consisting of a JASCO PU-2080 PLUS intelligent HPLC pump, a JASCO UV-2075 PLUS intelligent UV/Vis detector (254 nm), a JASCO RI-930 intelligent RI detector, and a JASCO CO-1565 intelligent column oven (23 °C) equipped with TOSOH TSK gel G6000H_{HR} and G3000H_{HR} columns (30 x 0.72(i.d.) cm) connected in series (eluent $CHCl_3$, flow rate 1.0 mL/min). Preparative SEC separation of dimers was performed using a JAI LC-908 preparative recycle chromatograph equipped with JAIGEL-1H and JAIGEL-2H columns connected in series (eluent $CHCl_3$). UV-vis absorption spectra were measured at room temperature with a JASCO V-550 and V-570 spectrophotometers. Steady-state emission spectra were taken on a JASCO FP-8500 fluorescence spectrophotometer. IR spectra were recorded on a JASCO FT/IR-6100 spectrometer using KBr pellet samples. Circular dichroism (CD) and linear dichroism (LD) spectra were taken with a JASCO-820 spectrometer. The spectra

were obtained by averaging those recorded at four (90^{o} interval) or two (180^{o} interval) different film orientations (angles) with the film face positioned vertically to the incident light beam for measurement. Linear dichroism contributions were thus minimized to afford true CD spectra. Differential scanning calorimetry (DSC) and thermal gravity analysis (TGA) were taken on Rigaku Thermo Plus DSC8230 and TG8120 analyzer at a heating rate of 10 K/min in nitrogen atmosphere. WAXD measurement was performed on a RIGAKU Miniflex diffractometer.

Computational method. Wave-form analysis of SEC curves for determination of the contents of polymers and dimers were performed using Origin 2018 software package (Origin Lab). Molecular mechanics structure optimization was conducted using the COMPASS force field implemented in the Discover module of the Material Studio 4.2 (Accelrys) software package with the Fletcher-Reeves conjugate gradient algorithm until the RMS residue went below 0.01 kcal/mol/Å. Molecular dynamic simulation was performed under a constant NVT condition in which the numbers of atoms, volume, and thermodynamic temperature were held constant. Berendsen's thermocouple was used for coupling to a thermal bath. The step time was 1 fs and the decay constant was 0.1 ps. Conformations obtained through MD simulation were saved in trajectory files at every 5 or 10 ps and were optimized by MM simulation.

References

(1) E. Yashima, N. Ousaka, D. Taura, K. Shimomura, T. Ikai and K. Maeda, *Chem. Rev.*, 2016, **116**, 13752-13990.

(2) E. Yashima, K. Maeda, H. Iida, Y. Furusho and K. Nagai, *Chem. Rev.*, 2009, **109**, 6102-6211.

(3) T. Nakano and Y. Okamoto, *Chem. Rev.*, 2001, **101**, 4013-4038.

(4) T. Nakano, *J. Chromatogr. A*, 2001, **906**, 205-225.

(5) Y. Okamoto and T. Nakano, *Chem. Rev.*, 1994, **94**, 349-372.

(6) J. Shen and Y. Okamoto, *Chem. Rev.*, 2015, **116**, 1094-1138.

(7) T. Nakano, *Chem. Rec.*, 2014, **14**, 369-385.

(8) R. Wang, Y. Zheng, X. Li, J. Chen, J. Cui, J. Zhang and X. Wan, *Polym. Chem.*, 2016, **7**, 3134-3144.

(9) Z. Yu, X. Wan, H. Zhang, X. Chen and Q. Zhou, *Chem. Commun.*, 2003, 974-975.

(10) J. Cui, J. Zhang and X. Wan, *Chem. Commun.*, 2012, **48**, 4341-4343.

Chapter 5. General Conclusions

Polymerization behavior and properties and structure of products with a focus on stereochemistry were investigated in detail for BINOL-14DIB, BINOL-13DIB, and BINOL-27DIB systems. In the BINOL-14DIB and BINOL-13DIB systems using BINOL at various e.e.'s, it was expected that chirality amplification effects may lead to single-handed helicity even at an e.e. of BINOL lower than 100%. In the case of BINOL-14DIB systems, a CD band at 295 nm based on polymer helicity was clearly separated from the CD bands below 250 nm based on BINOL unit chirality (at around 230 nm), and there was a clear, positive deviation of the intensity of the CD band at 295 nm at 25%, 50%, and 74% e.e. of BINOL in feed from the theoretical line connecting the CD intensity data point at 0% e.e. of BINOL and that at 100% e.e. of BINOL. This result meets the expectation, indicating that chirality is amplified in the BINOL-14DIB. Thus, even at an e.e. of BINOL lower than 100%, a highly biased helicity can be achieved. In the BINOL-13DIB system, CD bands based on polymer helicity appeared not be separated from the bands based on BINOL unit chirality, and chirality amplification effects thus could not be discussed.

The focus of the BINOL-27DIB system was to demonstrate an example of facile synthesis of chiral polyurethane bearing functional groups. Fluorene, the parent backbone of 27DIB, is an efficient fluorescent group, and poly(BINOL-alt-27DIB) was expected to be a material for CPL emission. The polymer indeed showed CPL emission whose sign was reversed for R-BINOL- and S-BINOL-based polymers while anisotropy of CPL (g_{lum}) was very low ($<10^{-5}$). Additionally, the selective formation of parallel and anti-parallel helices was unexpectedly attained. This aspect is intriguing and may deserve further,

detailed investigations because there has never been a clear example of such directional control of helix for synthetic helical polymer systems. This is a novel aspect of polymer stereochemistry that could lead to novel functional polymers. So far, the mechanism of the selection between parallel and anti-parallel helices is still not clear, and further studies would be necessary to shed light on this aspect.

Thus, it was clearly demonstrated in this thesis that helical polyurethanes can be prepared in a facile method where chirality amplification may facilitate efficient helix formation. In such syntheses, proper monomers need to be carefully selected also because stereochemistry of polymerization sensitively varies depending on chemical structure of the monomers as recognized for the 14DIB and 13DIB systems. In addition, functional groups can be readily introduced to such polymers simply by choosing a monomer based on functional chemicals; polyurethane can be a good platform for simple, facile synthesis of helical, functional polymers (Scheme 1). Embedding functional groups into the moieties connecting chiral diol-based units would be especially practical because a variety of chiral diols and polyols are available and diisocyanates can be easily prepared from diamines through reactions with triphosgene. I hope that this work would trigger research projects aiming at facile synthesis of chiral, functional polymers based on polyurethane backbone.

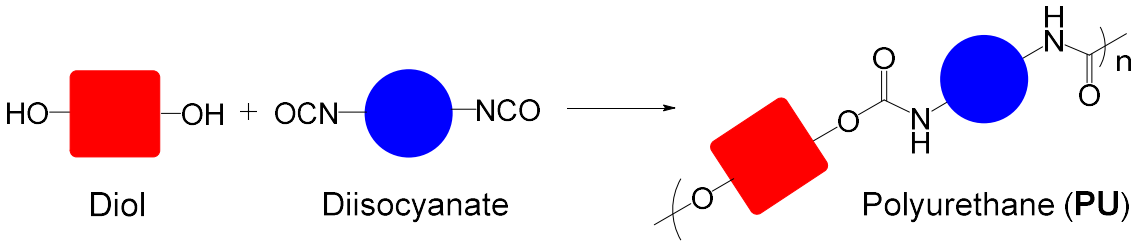

Scheme 1. Simple, modular synthesis of functional chiral polyurethanes.

Acknowledgment

I would like to express my appreciation beyond words to my supervisor, Prof. Tamaki Nakano (Macromolecular Science Research Division, Institute for Catalysis, Hokkaido University, Japan), who patiently guided in my thesis program and continuously provided me with stimulating ideas on science and warm encouragement.

I gratefully acknowledge Prof. Takanori Suzuki, Prof. Masaya Sawamura, and Prof. Toshifumi Satoh for their reviewing my thesis and giving me helpful advises on it.

I express my gratitude to Prof. Dr. Yoshitane Imai (Kindai University, Japan), Prof. Dr. Takunori Harada (Oita University, Japan), and Prof. Adriana Pietropaolo (Università di Catanzaro, Italy) for their kind collaboration and helpful advice and for their valuable comments on the thesis work.

I am thankful to Dr. Zhiyi Song and Dr. Yue Wang of Nakano Laboratory for their experimental assistance and wish to thank all members of Nakano Laboratory of Hokkaido University for their friendship and encouragement.

Finally, I acknowledge my beloved parents, Shanwei Dai and Meiyu Yang, and all family members for encouragement and support.

March 25, 2020

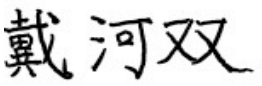

Heshuang Dai